Master's Thesis

Efficient Perovskite Nanocrystals Based Light-Emitting Diodes with Hole Transport Layer Modification

Hyeon Seo Kim

School of Energy and Chemical Engineering
(Energy Engineering)

Ulsan National Institute of Science and Technology

2021

Efficient Perovskite Nanocrystals Based Light-Emitting Diodes with Hole Transport Layer Modification

Hyeon Seo Kim

School of Energy and Chemical Engineering
(Energy Engineering)

Ulsan National Institute of Science and Technology

Efficient Perovskite Nanocrystals Based Light-Emitting Diodes with Hole Transport Layer Modification

A thesis/dissertation submitted to
Ulsan National Institute of Science and Technology
in partial fulfillment of the
requirements for the degree of
Master of Science

Hyeon Seo Kim

11/19/2020 of submission

Approved by

Advisor
Jin Young Kim

Efficient Perovskite Nanocrystals Based Light-Emitting Diodes with Hole Transport Layer Modification

Hyeon Seo Kim

This certifies that the thesis/dissertation of Hyeon Seo Kim is approved.

11/19/2020 of submission

Signature

Advisor: Jin Young Kim

Signature

Myoung Hoon Song

Signature

Gi-Hwan Kim

Abstract

My MS research has focused on light-emitting diodes (LEDs) devices based on perovskite nanocrystals (PeNCs). All-inorganic PeNCs are promising material for optoelectronic devices due to their easily tunable bandgap, narrow full width at half maximum (FWHM), and high photoluminescence (PL) quantum yield. Moreover, all-inorganic perovskite material has better stability than the other perovskite material that employs hybrid or organic part at A site of perovskite. These outstanding physical properties caused lot of interest in PeNCs for LEDs devices. To make highly efficient LEDs devices, there are several important factors. Those are smooth film morphology, energy band alignment for low charge injection barrier, and charge balance between hole and electron. Especially, perovskite material has low exciton binding energy (E_b), therefore, confining electron and hole into nanocrystals is very important to make exciton. By considering these factors, a lot of research is going on. However, blue-emitting PeNCs have resulted lower quantum yield compared to red or green-emitting PeNCs due to their large bandgap and anion segregation. To achieve commercialization of PeNCs for future display, white LEDs are indispensable, therefore, great development of blue-emitting LEDs is required. From this point of view for high-efficiency blue LEDs devices, 1,8-diiodooctane (DIO) additive has been used for our research. DIO is added to poly[bis(4-phenyl)(4-butylphenyl)amine] (poly-TPD) solution that is employed in hole transporting layer (HTL) to improve hole injection and passivate trap states between poly-TPD layer and perovskite NC layer. By adopting DIO additive to HTL, external quantum efficiency (EQE) of green PeNCs LEDs was enhanced from 2.89 % to 5.17 % compared to the reference device, and EQE of blue PeNCs LEDs was enhanced from 0.58 % to 1.34 % compared to the reference device.

Contents

List of Figures

Figure 3.11d The EQE of blue EL device according to the different volume fraction of DIO to poly-TPD solution.

List of Tables

List of Abbreviation

LEDs Light-emitting diodes

PeNCs Perovskite nanocrystals

FWHM Full width at half maximum

DIO Diiodooctane

Poly-TPD Poly[bis(4-phenyl)(4-butylphenyl)amine]

HTL Hole transport layer

EQE External quantum efficiency

BLU Backlight unit

OLEDs Organic light-emitting diodes

EL Electroluminescence

RGB Red, Green, and Blue

Alq_3 Tris(8-hydroxyquinolinato) aluminium

LEDs Light-emitting diodes

NCs Nanocrystals

PeLEDs Perovskite light-emitting diodes

ITO Indium tin oxide

CF Chloroform

HBr Hydrogen bromide

PEA phenylethyl ammonium

QDs Quantum dots

$MAPbBr_3$ Methyl ammonium bromide

PeQDs Perovskite quantum dots

LARP Ligand-assisted reprecipitation

PeQLEDs Perovskite Quantum dots light-emitting diodes

$CaTiO_3$ Calcium titanium oxide

FA Formamidinium

EA Ethyl ammonium

VBM Valence band maximum

CE Current efficiency

PE Power efficiency

SI System of Units

HOMO The highest occupied molecular orbital

LUMO The lowest unoccupied molecular orbital

PFI Tetrafluoroethylene-perfluoro-3,6-dioxa-4-methyl-7-octenesulfonic acid copolymer

SCLC Space-charge-limited-current

RbI Rubidium iodide

PFN Poly[(9,9-bis(3′-(N,N-dimethylamino)propyl)-2,7-fluorene)-alt-2,7-(9,9-dioctylfluorene)]

TCSPC Time-correlated single-photon counting

CB Chlorobenzene

DEE Diethyl ether

TPBi 2,2′,2″-(1,3,5-benzinetriyl)-tris(1-phenyl-1-H-benzimidazole)

PMA Phenylmethylamine

PLQY Photoluminescence quantum yield

TEM Transmission electron microscopy

BHJ Bulk heterojunction

LiF Lithium fluoride

Al Aluminium

AFM Atomic force microscopy

Rq Root-mean square

Chapter 1
Introduction

1.1 Optoelectronic device

These days, the demand for many kinds of energy is rapidly increasing and there are many sources of the energy such as oil, coal, gas, and nuclear power. These energy consumption by energy source is shown in **Figure 1.1**. However, those energy sources are not suitable for the future energy harvest due to its environmental problem and riskiness. Although those sources have possessed lots of part of energy harvest so far, such trend is now shifting to carbon-free, safe, and renewable energy source such as wind energy, tidal energy, hydroelectric energy, and solar energy. Especially, solar energy aroused much interest from the study since it well coincides with the future energy. Solar energy does not make byproduct like CO_2. It means that solar energy is carbon-free clean energy source and does not harm earth's environment. Also, it is infinite energy source which can be used for a long time. With these many advantages, the numerous research projects on the solar cells have been progressed from 1950s. As a result, silicon solar cells are already commercialized and to replace silicon solar cells, a lot of research are going on such as organic solar cells and perovskite solar cells. However, there are several ways to use the electrical energy which is from solar energy through other optoelectronic devices. One of them is LEDs which can produce the light with target wavelength from the electricity. Since using the energy efficiently can be also the same effect with producing the energy, those optoelectronic devices are in a lot of spotlight for the future energy harvest and application.

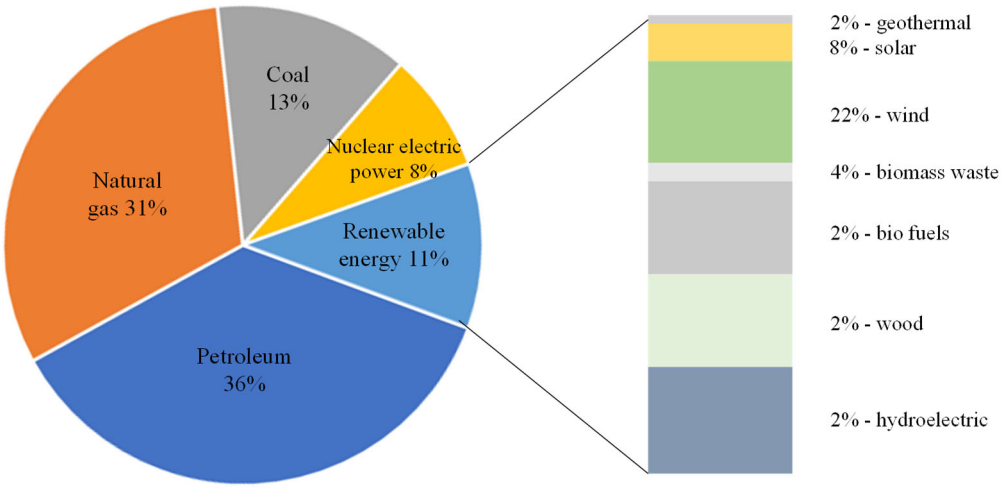

Figure 1.1 U.S. primary energy consumption by energy source in 2018 including renewable energy.

1.2 LEDs Device

The LEDs device is like the solar cells device in that it is operated by hole and electron but there is a difference in that LEDs device works opposite to the solar cell device. In solar cell, electrical energy is produced by the light energy generally from the sun. It means that light energy generates electron-hole pairs which can be also called excitons and then, generated charge carriers are separated to electrodes on both sides. On the contrary, in LEDs, electrical energy is transformed to the light energy in the form of photons. Both charge carriers are injected to the emission layer from electrodes by applied voltage and then, recombination of them produces exciton to release the light energy. To enhance the efficiency which means the ratio of the number of photons to the number of electrons injected, there is much research going on.

As the technology to produce the energy advances, it is also important to make the devices that can efficiently use the energy produced. One of them is the LEDs devices and nowadays, everyone sees the world through the display. Until now, liquid crystal display (LCD) has been widely used for display at television or cell phone. However, the LCD has several shortcomings for the future display. The LCD has many components including backlight unit (BLU), thin film transistor (TFT), liquid crystal, and polarizers. These many indispensable components of LCD make it more difficult to realize thin display panel. Also, because of the existence of the BLU, it has a limit to make flexible mobile display and to make high definition. For these reasons, industrial trends are shifting from LCD to organic LEDs (OLEDs). First, OLEDs is easy to make thin due to its simple structure compared to LCD. Second, OLEDs is suitable for high-definition large-scale display and make light spontaneously. Lastly, OLEDs operates necessary pixel only, therefore, power consumption can be reduced. For these advantages, markets are launching television, cell phone, or smart watch with OLEDs panel and many studies have been conducted on OLEDs. Comparison of display structure between LCD and OLEDs is shown in **Figure 1.2**. However, there are also many drawbacks of OLEDs. Basically, OLEDs employs organic material such as poly(p-phenylene vinylene) (PPV) or polyfluorene.[1] It makes difficult to produce OLEDs panel due to its high unit cost of production. Also, these organic substances are vulnerable to moisture, therefore, encapsulation process is indispensable for device stability. Moreover, there is unavoidable burn-in phenomenon due to the blue organic material. For these reasons, new innovative material for the LEDs has been on a research. One of them is perovskite since it has cheap cost compared to OLEDs and higher color purity. In addition, perovskite material is easy to tune the wavelength by simply mixing the components or control the grain size.

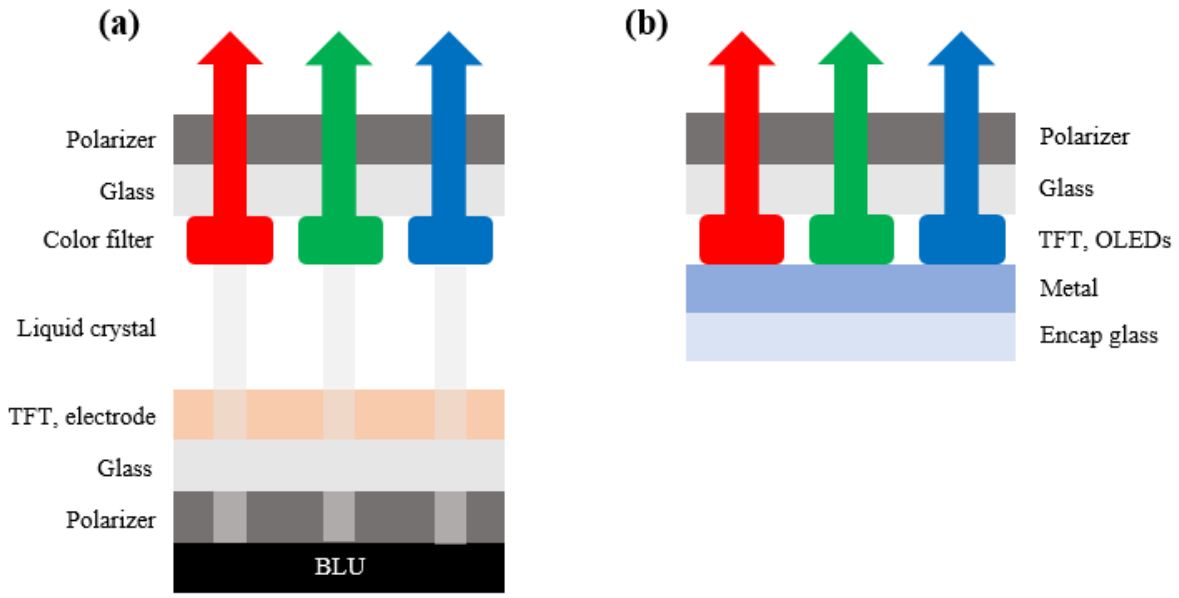

Figure 1.2 The comparison of display structure between (a) LCD and (b) OLEDs

1.3 History of LEDs device

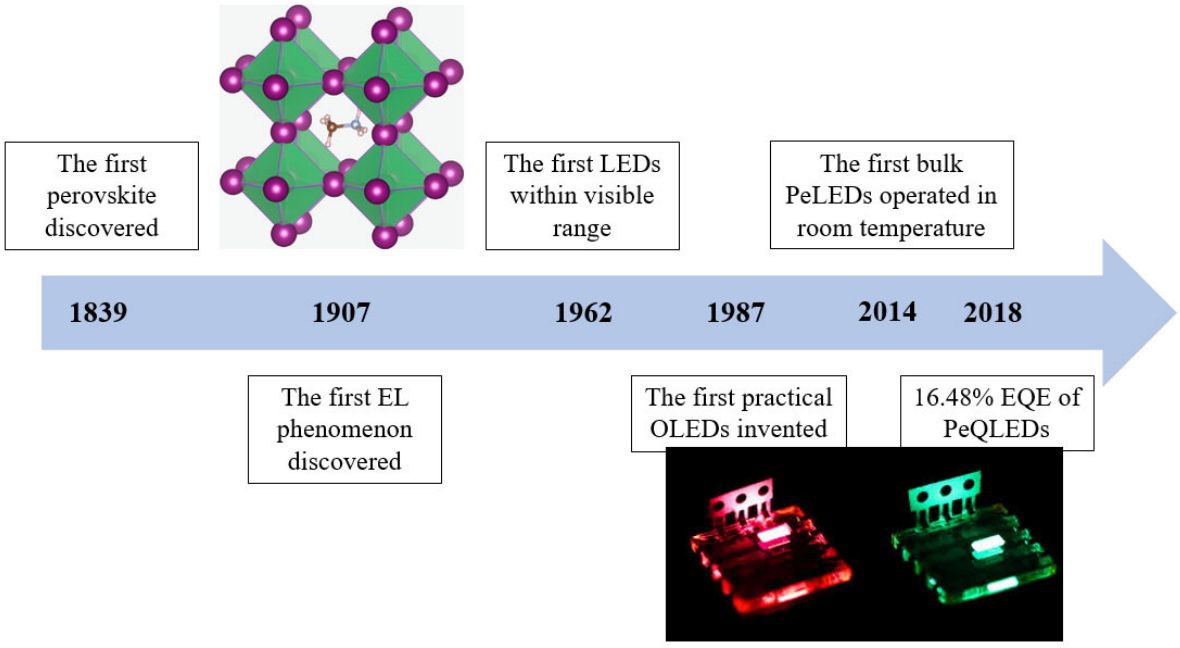

Figure 1.3 The rough timeline of history of perovskite and the development of PeLEDs

Electroluminescence (EL) is a phenomenon in which light is emitted by a material that is subjected to an electric field.[2] The first discovery of EL was by H. J. Round of Marconi Labs in 1907. After EL phenomenon discovered, there has been many results of making LED device regardless of the wavelength. The first LEDs device which emits the light in visible-range red spectrum was demonstrated based on GaAsP by Nick Holonyak in 1962.[3] Based on this invention, three primary colors LEDs which are red, green and blue (RGB) LEDs devices have been studied to apply the LEDs devices to the commercial area such as TV or cellphone. Among them, blue LEDs devices are the biggest obstacle because of the stability issue containing burn-in phenomenon, therefore, related research had been studied based on the inorganic materials such as InGaN or AlGaN. Around the same time, Martin Pope and his co-workers in France primally reported EL which was based on a single crystal of anthracene in 1963. Also, he suggested the structure of electrode contact that is needed to inject hole and electron and, it became fundamentals of charge injection in modern OLEDs devices. However, high operating voltage and lower efficiency compared with inorganic LEDs as mentioned above were the problems of those organic crystal-based LEDs devices, therefore, research was mainly focused on the inorganic materials in the initial stage. Meanwhile, in 1987, Tang and Van Slyke first reported practical OLEDs that is consist of bilayer structure.[4] One is for hole injection and the other is for electron injection. It showed lower operating voltage and improved efficiency compared with previous OLEDs. After the practical OLEDs reported, various materials including small molecules, polymer, and phosphorescent materials have been used for emission layer of OLEDs. Tang *et al*. used tris(8-hydroxyquinolinato) aluminium (Alq_3) as a small molecule to make OLEDs in 1987.[4] Burroughes, J. H. *et al*. reported a green OLEDs using PPV in 1990.[1] Forest, S. R. *et al*. added iridium complex which was tris(2-phenylpyridine) iridium ($Ir(ppy)_3$) to poly(N-vinylcarbazole) to make EL emission in 1999.[5] Despite those considerable progress, several disadvantages and challenges have made the demand of new paradigm of LEDs device.

1.3.1 History of perovskite LEDs device

While the research of OLEDs being retarded, perovskite materials rose to the new source of LEDs devices. Perovskite can be classified according to their dimensions and those are 3D bulk, 2D layered, and nanocrystals (NCs).

At the first, in 2014, Tan *et al*. reported 3D bulk halide perovskite LEDs (PeLEDs) device for the first time.[6] They fabricated infrared LEDs device at 750 nm of wavelength with an indium tin oxide (ITO)/TiO2/$CH_3NH_3PbI_{3-x}Cl_x$/F8/MoO3/Ag structure. Although the performance of the device was low, they suggested a new direction of LEDs device. Also, one of the achievement of 3D bulk PeLEDs film fabrication was reported in 2015 by T. W. Lee group. They introduced nanocrystal pinning (NCP)

technology instead of normal spin coating. Chloroform (CF) was introduced to the spin coating process with original good solvent and CF made perovskite got fast crystallization to reduce the grain size.[7] In addition, Hydrobromic acid (HBr) was added to the perovskite precursor solution to increase the solubility of the precursor by Yu et al. group. This technology made crystallization rate slow and the film morphology was enhanced.[8]

Next, 2D layered perovskite which was layer-controllable for applying it to LEDs device was reported by Mitzi *et al*. in 1994.[9] With this report, the paper about the first EL by 2D layered perovskite was published by Era and coworkers in the same year but their device was not practical since the device was operated at liquid nitrogen temperature.[10] Meanwhile, Yuan *et al*. reported precisely layer-controllable of 2D perovskite by varying the amount of phenylethyl ammonium (PEA) ligand.[11] This report revealed the relation between the amount of ligand and dimension of perovskite, also, suggested the existence of multi-phase of 2D perovskite according to the degree of proximity to 2D structure and energy funneling effect. Since its structure contains multi-phase which means there are 3D bulk phase and 2D sheet-like phase, it was also called quasi-2D perovskite structure. Inspired from this report, Ban *et al*. reported the 2D perovskite LED device with EQE exceeding 15 % by utilizing energy funneling effect and it could be done due to the multi-phase of 2D perovskite.[12]

Finally, the last category is quantum dots (QDs) or NCs which mean zero-dimension. The concept of QD for quantum confinement effect was had been existed such as CdSe(ZnS) core(shell) QD, however, the first PL by perovskite QD was observed in 2012 by Kojima *et al*.[13] They reported green PL using methyl ammonium lead bromide ($MAPbBr_3$) spin coated onto mesoporous Al_2O_3, however it was technically perovskite nanoparticles between mesoporous Al_2O_3, not pure perovskite QDs (PeQDs), and it was hard to apply to the device due to the limit of substrate. Therefore, to synthesize the pure PeQDs, two main methods have been suggested, and those are ligand-assisted reprecipitation (LARP) at room temperature and hot-injection method. In 2015, Kovalenko group reported hot-injection synthesis method which injects one precursor solution to the other precursor solution under high temperature condition.[14] Around the same time, Zhang *et al*. reported LARP synthesis method which did not require high temperature and N_2 atmosphere.[15] With those reports, the first all-inorganic PeQDs LEDs (PeQLEDs) device was fabricated by Song *et al*.[16] The device showed EQE and maximum luminance of 0.12 % and 946 cd/m^2 at 514 nm. Though its performance was not outstanding, it suggested the new candidates for the future LEDs technology. After those research, EQE of PeQLEDs has increased from 0.12 % to 16.48 % in 3 years.[17] In 2018, Zeng group reported organic-inorganic hybrid passivation PeQLED with an EQE of 16.48%.[17]

Thus, various class of PeLEDs has been developed for efficiency and stability, and its results confirmed that perovskite is one of the best candidates for the future LEDs emission layer.

Chapter 2

Theoretical & Mathematical Development

2.1 Perovskite

In 1839, Gustav Rose found calcium titanium oxide ($CaTiO_3$) in Ural Mountain in Russia and that material was the first material which was based on the perovskite structure. After that, Lev Perovski clarified the perovskite structure and gave the name of perovskite to these ABX_3 group. Therefore, any materials that have the same crystal structure with CaTiO3 is called perovskite materials since then, and it is shown in **Figure 2.2**. Meanwhile, Victor Goldschmidt suggested tolerance factor to precisely define the perovskite structure.[18] The formula of Goldschmidt tolerance factor is as follows.

$$t = (R_A + R_X)/\sqrt{2}(R_B + R_X)$$

Here, R_A, R_B, and R_X are effective ion radii of A, B, and X element, also, these are also expressed in **Figure 2.1**.[18] To call a material as perovskite, *t* value should be within 0.8-1.1. Especially for cubic perovskite, *t* value is within 0.9-1, and if *t* value is over 1, the structure gets little distorted, so it becomes hexagonal or tetragonal due to too big A site ion or too small B site ion. If *t* value is within 0.71-0.9, orthorhombic or rhombohedral structure are generated. Since the closer *t* value to 1, the more stable perovskite structure is, by using this factor, proper element or material can be selected to fit cubic perovskite structure. As a result, many materials have been tried at each sites such as Cs, MA, formamidinium (FA), ethylammonium (EA) at A site, Pb^{2+}, Sn^{2+}, Ge^{2+} at B site, and Cl, Br, I at X site.

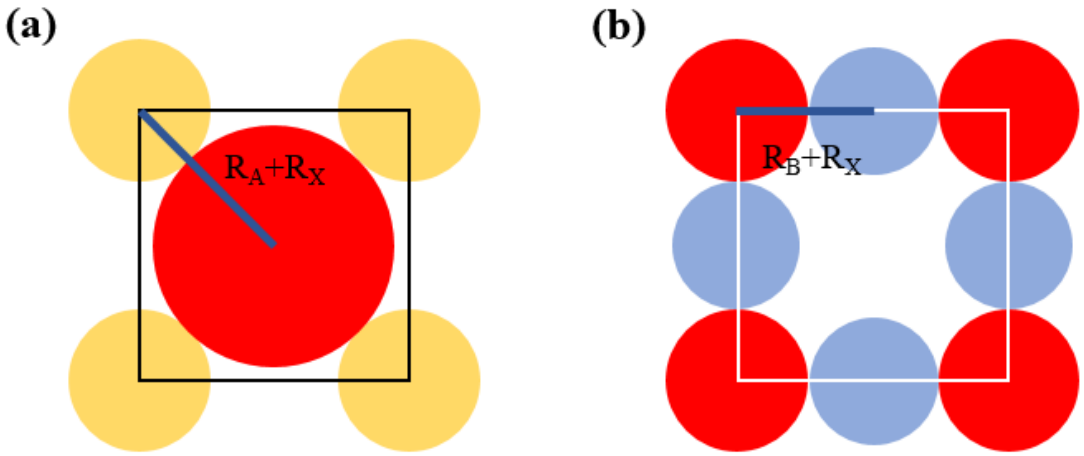

Figure 2.1 Goldschmidt tolerance factor; (a) R_A+R_X, (b) R_B+R_X.

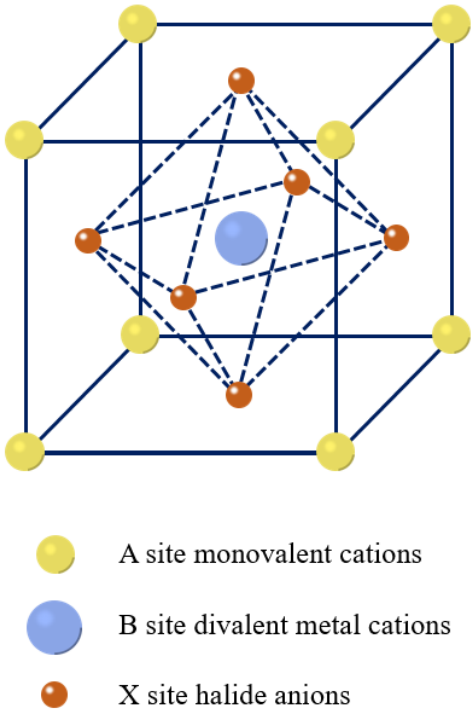

Figure 2.2 The rough timeline of history of perovskite and the development of PeLEDs

First, when the A site is considered, the size of cation influences crystal structure since the cation can affect to the bond length of B-X octahedra. Therefore, the size of the A site cation has important role of determining the bandgap of perovskite. The A cation sizes are $R_{FA}>R_{MA}>R_{Cs}$ and when the size of cation increases, the bandgap of perovskite becomes smaller.[19] The relation between the size of the A site cation, ionic radii, and the bandgap of $APbI_3$ is on the table 2.1.[19-22]

A site cations	FA	MA	Cs
Ionic radii (Å)	1.9-2.2	1.8	1.67
Bandgap of $APbI_3$ (eV)	1.34-1.48	1.51-1.55	1.73

Table 2.1 The relation between the size of the A site cation, ionic radii, and the bandgap of $APbI_3$

In addition, as mentioned above, making Goldschmidt tolerance factor close to 1 for stable cubic perovskite structure is very important for the stability. At this point of view, mixing A site cation is one of the good strategy for stable perovskite such as Cs/Rb, MA/FA, or Cs/FA.[23-26]

Second, B site cations such as Pb^{2+}, Sn^{2+}, Ge^{2+} construct central octahedra with halide anion. The difference of electronegativity between B and X site ions has important role of determining the bandgap

of perovskite. Due to this reason, $MAPbX_3$ has larger bandgap which is within 1.6-1.8 eV than $MASnX_3$ which is within 1.2-1.4 eV.[27-29] Meanwhile, most of research have focused on Pb^{2+} for the B site ion since it has better stability than Ge^{2+} or Sn^{2+}. Ge^{2+} is unstable due to 2+ oxidation state and Sn^{2+} is easily oxidated to Sn^{4+} when it is exposure to air.[28-31] However, Pb has toxicity and it is expected to have lower photocurrent density than Sn, therefore, there have been many study about replacing B site ion.[32]

Third, X site halide anion such as Cl, Br, or I most directly involved in the decision of the bandgap of perovskite. The ionic radii show increasing tendency from Cl to Br to I, and valence band maximum (VBM) of perovskite also changes from 3p to 4p to 5p. The tendency of the ionic radii is shown in **Table 2.2**. Due to this reason, the bandgap of perovskite is decreasing as its halide composition moves from Cl to Br to I. In other words, emission spectra of perovskite are getting red-shifted according to the above tendency.[14, 33-35] In iodine case, since I and Pb well match on covalent character, $APbI_3$ has most stable crystal structure. Nevertheless, mixing halide components is widely used to tune the bandgap of perovskite. There are many cases that mixed halide components such as I/Cl, I/Br, or Br/Cl.[36-39] However, if halide components are mixed, halide anion segregation of the same components are observed under illumination or charge-carrier injection. This is caused by ion migration. As a result, EL peak shift or efficiency drop was inevitably accompanied with the halide anion segregation progressed. To overcome this obstacles, several research on preventing the halide segregation were reported.[40] It is hot research area of perovskite solar cells and LEDs to make combination of A, B, and X site while the perovskite structure is maintained which is related to Goldschmidt tolerance factor.

X site anions	I	Br	Cl
Ionic radii (Å)	2.2	1.96	1.81

Table 2.2 The ionic radii of X site anions which contain I, Br, and Cl.

2.2 OLEDs to PeLEDs

OLEDs has been considered as fascinating research field due to its contrast ratio, power efficiency, thickness, and probability of compatibility with flexible substrates. However, at the same time, OLEDs has several disadvantages. First, organic material is easy to be degraded when it is exposure to oxygen, moisture, or UV light, and it leads the device to have short lifetime. Second, blue OLEDs has lower efficiency compared with red or green OLEDs and it makes hard to make white OLEDs. Third, production cost of OLEDs is high due to its manufacturing process and organic materials. To improve those shortcomings of OLEDs, many research has been studied such as encapsulation or layer printing technology. Meanwhile, researchers started to deal with perovskite materials as emission layer of LEDs devices since there are many advantages when the perovskite materials are used for LEDs device

compared to existing organic emission materials. First, as mentioned above, bandgap can be easily tuned by changing halide component ratio, therefore, the color of LEDs device can be easily varied from blue to red within visible region.[38] Second, PeLEDs shas a high color purity compared to OLEDs. It can be easily confirmed by narrower FWHM of PeLEDs (~20 nm) than OLEDs (40 nm~), as shown in **Figure 2.3**.[41-44] Also, perovskite materials generally have low cost compared to organic materials. Finally, device fabrication process of PeLEDs is simpler than OLEDs since PeLEDs can be fabricated by solution-processed method such as spin coating but in OLEDs industry, thermal evaporation is essential due to its film morphology.[45] In research area, several report about solution-processed OLEDs device have been published but there is limitation such as solvent choice or device structure.[46]

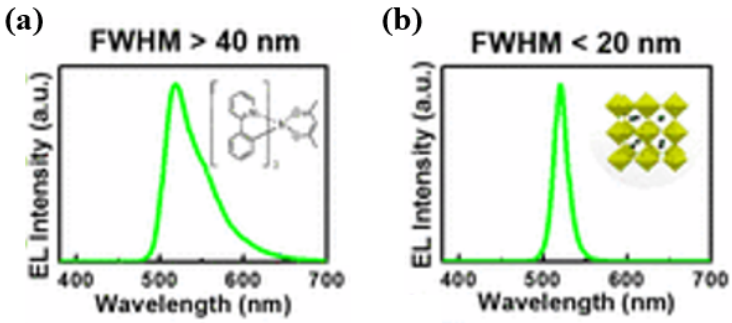

Figure 2.3 General FWHM of (a) OLEDs, and (b) PeLEDs.[72] Copyright 2016, Proceedings of the National Academy of Sciences of the United States of America (PNAS)

2.3 PeLEDs Device

This chapter will introduce basic working mechanism of PeLEDs and how to characterize LEDs devices. Based on well-understood working mechanism, many idea for enhancing parameters of PeLEDs can be suggested by manipulating properties of the device or NCs.

2.3.1 Working mechanism of PeLEDs

PeLEDs generally consist of both electrodes which are anode and cathode, charge carrier transporting layer such as HTL and electron transporting layer (ETL), and emission layer which is perovskite here. The charge carriers should recombine each other radiatively to make light by the LEDs device, following 4 steps are required.

Step 1. Charge injection

Step 2. Charge transport

Step 3. Radiative recombination

Step 4. Light emission

To operate the LEDs device, basically, electron and hole should be injected from both electrodes (step 1). Then, injected these charge carriers are transported through HTL and ETL to emission layer which is perovskite here (step 2). These transported hole and electron are recombined in emission layer. In other words, electron is relaxed to ground state to make exciton (step 3). In that process, energy from the relaxation is produced and among many kinds of the energy form, a portion of light energy is emitted by photon (step 4). These steps are shown in **Figure 2.4**.

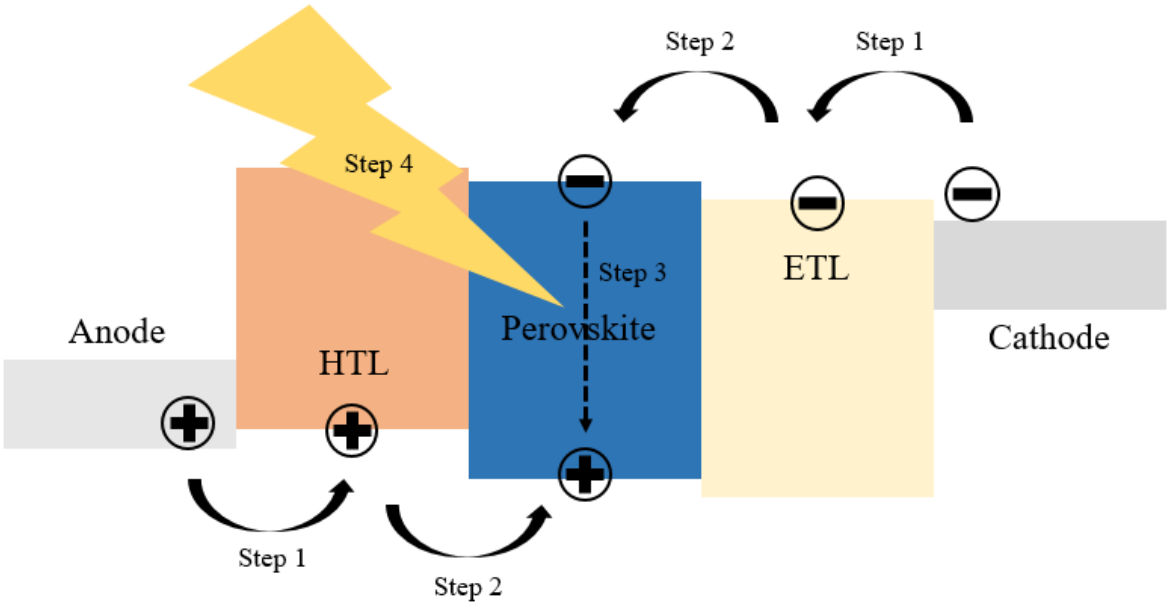

Figure 2.4 The working mechanism of LEDs including step 1 (charge injection), step 2 (charge transport), step 3 (radiative recombination), and step 4 (light emission).

As seen in Figure 2.4, mechanism of LEDs is opposite to solar cells. Solar cells extract charge carriers from the active layer, but LEDs inject charge carriers and makes them recombine to form exciton. However, perovskite has small exciton binding energy (50 meV) and high dielectric constant (ε_r~30).

It is advantages for solar cells, but on the other hand, shortcomings for LEDs device. For LEDs device, it is important to confine charge carriers to the perovskite crystals, therefore, manipulation such as decreasing grain size or dimension of perovskite is needed to make excitons.

2.3.2 Parameters of PeLEDs

To measure the performance of LEDs device, there are many parameters such as EQE, current efficiency (CE), power efficiency (PE), luminance, FWHM, and turn-on voltage. Among them, EQE is most important factor which describes LEDs performance. EQE is defined as the ratio of the number of the photon emitted from the LEDs device to the number of electrons injected to the device and it is given in the following equation.

$$\eta_{EQE} = \eta_{outcoupling} \cdot \gamma \cdot \phi = \frac{the\ number\ of\ emitted\ photons}{the\ number\ of\ injected\ electrons} \times 100 \quad (2.1)$$

Where A is outcoupling factor and B is balanced charge injection factor, and C is radiative quantum efficiency. Although A is low because of optical loss due to high refractive index, several studies recently reported about reducing optical loss. To enhance B, proper choice or combination of HTL and ETL should be accompanied. Finally, radiative quantum efficiency is related to the defect site and charge confinement, therefore, it is important to passivate those defect sites and confine charge carrier into the perovskite NCs.

Luminance (cd/m2) of LED is expressed as candela (cd) per square meter where cd is one of the international System of Units (SI). Nit is the same unit with cd/m2 for expressing luminance.

CE (cd/A) is defined as the ratio of luminance to current density and is given in the following equation.

$$CE\ (cd/A) = \frac{luminance\ (cd/m^2)}{current\ density\ (mA/cm^2)} \times 10^{-1} \quad (2.2)$$

PE is defined as the ratio of emitted power to the injected power and is given in the following equation. When current is constant, PE is increased as injected voltage is decreased and it means the charge injection barrier of LEDs.

$$PE\ (lm/W) = \frac{\pi \times luminance\ (cd/m^2)}{voltage\ (V) \times current\ density\ (mA/cm^2)} \times 10^{-1} \quad (2.3)$$

FWHM is a width between the independent variable of a function when dependent variable is half of its maximum value. For characterizing LED device, FWHM is used to express color purity. As FWHM becomes narrower, emission wavelength gets more specified. It means that the color purity is increased. Its units are eV or nm and for perovskite materials, it is usually under 20 nm.

Turn-on voltage means the voltage which can sufficiently operate the LED device and it is about 3-4V

for green PeLEDs device and 2 V for red PeLEDs device. It is related to the bandgap of emission layer and it can be decreased if charge balance and charge injection are enhanced. It can be realized by using interlayer which has high mobility or designing proper device structure for good energy band alignment or balancing charge injection through both interlayer. It is also important factor for the increased stability and reduced power consumption of the LEDs device.

2.3.3 Properties of PeLEDs

There are many properties which characterize LEDs device and its performance. Among them, the structure of device is the most basic thing to define the device. Basically, LEDs device consists of both electrodes which are anode and cathode, charge transport layer, and the emission layer which is perovskite for PeLEDs device. Each of layer has intrinsic the highest occupied molecular orbital (HOMO) and the lowest unoccupied molecular orbital (LUMO) that determine the bandgap of such material. Various materials which can be used as HTL, ETL and emission layer is shown in **Figure 2.5**. Then, the energy level difference between adjacent layer represents the energy barrier of charge injection. Therefore, if the energy barrier is lower, it gets easier to inject the charge carrier. According to this, there has been many reports about adding interlayer to reduce the energy barrier.[48-51] For halide PeLEDs, Kim *et al*. were the first group who deal with interlayer modification.[47] Before self-organized buffer HIL (Buf-HIL) which consists of PEDOT:PSS, perfluorinated polymeric acid, and tetrafluoroethylene-perfluoro-3,6-dioxa-4-methyl-7-octenesulfonic acid copolymer (PFI) was introduced, the energy barrier between PEDOT:PSS and perovskite layer was very large and EQE was extremely low at 0.000393 %. But after the Buf-HIL was introduced, work function was tuned from 5.2 eV to 5.95 eV and EQE was enhanced by over 300-fold. It is attributed to blocking electrons and reducing exciton quenching at the interface between HIL and perovskite layer. Also, in LEDs device, it is important to confine charge carriers in the emission perovskite layer to make them recombined by producing exciton. Therefore, interlayer can act as a charge carrier blocking layer also. HTL should block electron and ETL should block hole.[52] However, too many interlayer inevitably accompanies many interfaces between the layer, and it induces charge trap states. It is important to consider the drawback of interlayer modification.

Except for the energy band alignment, mobility enhancement is also one of the goal of interlayer modification. Though there are many materials which have similar bandgap as shown in **Figure 2.5**, there are a few materials that researcher commonly use. The mobility of materials is also related to the charge injection and the mobility can be calculated by fitting the space-charge-limited-current (SCLC) region with Child's law which is defined as follows.[53]

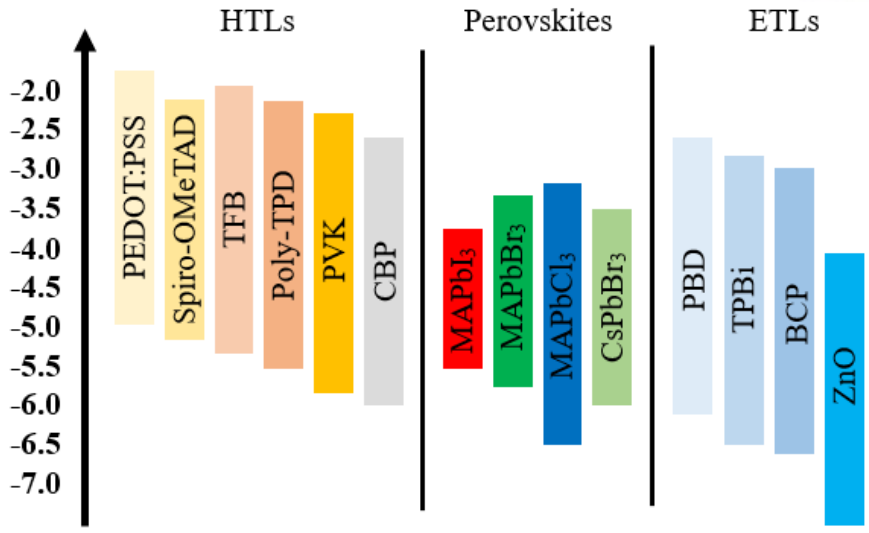

Figure 2.5 Energy band alignment including HOMO and LUMO level of various materials used as HTL, perovskite layer, and ETL in the reported PeLEDs.

$$J = \frac{9}{8}\varepsilon_0\varepsilon_r\mu\frac{V^2}{D^3} \quad (2.4)$$

where J is the measured current density, ε_0 is vacuum permittivity, ε_r is relative permittivity, V is driving voltage, μ is the mobility of material, and D is the thickness of layer. After ohmic region where current is linearly increased as voltage injection, SCLC region where the current is proportional to square of the voltage appears. When the number of injected charge carrier is greater than thermally generated charge carrier, total current is governed by injected charge carrier, and SCLC flows. At this region, transition time becomes shorter than relaxation time of charge carrier, and *J-V* characteristics follow the Child's law. Therefore, by measuring *J-V* relationship of specific layer, the mobility of the layer can be calculated. Zou et al. compared the mobility of PVK and poly-TPD which are used as HTL, and fabricated LEDs device which had better EQE.[48] Also, manipulation such as using an additive for enhanced mobility is also one of the method to increase the device efficiency.[54-55] Turren-Cruz et al. used rubidium iodide (RbI) as an additive to perovskite active layer and it showed enhanced carrier mobility and improved efficiency.[55]

However, if the charge carrier balance between hole side and electron side does not match despite high carrier mobility, the efficiency of LEDs device must be low. In other words, if excess charge carrier is accumulated at the interface of perovskite or inside of perovskite layer, not only it affects to the stability of perovskite crystals but also recombination rate is not increased. Therefore, it is important to balance charge carrier injection from both electrodes.[56] Shin *et al.* introduced poly[(9,9-bis(3′-(N,N-dimethylamino)propyl)-2,7-fluorene)-alt-2,7-(9,9-dioctylfluorene)] (PFN) with halide ions between

HTL and perovskite layer to make well-balanced charge carrier.[57] By making single carrier device, charge injection from both electrodes can be confirmed and charge balance can be verified.

Next, one of the crucial things of LEDs device is recombination of hole and electron to make exciton. At this time, charge carriers can properly recombine at emission layer but if there are trap states at interface or surface and defect states at perovskite crystals, non-radiative recombination can occur. To analyze the ratio of radiative recombination and non-radiative recombination, time-correlated single-photon counting (TCSPC) is used. After exciting electron by light, equipment observes the decay of excited electron. Then, fast decay (τ_1) and slow decay (τ_2) are related to non-radiative trap-assisted recombination and radiative recombination, respectively. By measuring these factor, the ratio of radiative to non-radiative recombination can be calculated. Also, average PL lifetime (τ_{Avg}) can be calculated from each decay time and the ratio according to the following equation

$$\tau_{Avg} = \tau_1 \cdot f_1 + \tau_2 \cdot f_2 \quad (2.5)$$

where f_1 and f_2 are percent contributions of each decay's lifetime. Based on this, when particularly perovskite emission layer is manipulated, many reports include TCSPC analysis to show increased proportion of radiative recombination and longer average PL lifetime which indicate decreased concentration of trap states.[58] One of them analyzed that the high f_1 was due to increased surface defect sites. Nevertheless, longer slow decay time compared to pristine sample was due to less defects inside the bulk perovskite phase.[58]

In addition, film morphology is one of the most important constituent for well-fabricated device. If film morphology is bad, trap or defect states must be generated at the surface between layers and it affects to the efficiency of device and charge injection to the emission layer, therefore, the film morphology is related to optical and electrical properties of LEDs device.[8, 50, 51, 59] As a result, fabricating a uniform pinhole-free perovskite layer or interlayer is important.[60] The film morphology is affected by substrate, layer deposition process such as material composition, spin coating condition, annealing condition, solvent treatment, and additive. Representative additive to perovskite layer is acid. The acid helps inorganic perovskite precursor well dissolved in solvent and decreased crystallization rate induces uniform and full-covered perovskite layer.[59] Thermal annealing is also essential for making device since it increases perovskite crystallinity and film quality. Enhanced crystallinity is also related to the stability of device. However, optimizing proper annealing temperature and time is needed,
because excessive annealing condition can produce discontinuous morphology or crack which can generates leakage current. By optimizing annealing condition, several reports about increasing device stability have been published.[61-62] Finally, solvent engineering can be the method for better morphology. The series of solvent which do not dissolve the perovskite precursor such as toluene, chlorobenzene (CB), diethyl ether (DEE) can be used during spin coating of perovskite layer. Those solvent are called

anti-solvent and Seok *et al*. adopted anti-solvent treatment, and that treatment rapidly removed polar solvent and simultaneously made perovskite be crystallized. Then, they obtained enhanced film quality and better morphology. Also, for PeLEDs, solvent treatment with 2,2′,2″-(1,3,5-benzinetriyl)-tris(1-phenyl-1-H-benzimidazole) (TPBi) or phenylmethylamine (PMA) was applied to the perovskite layer.[7, 63]

Stability of LEDs device is also rising issue. Although EQE of PeLEDs device has been developed over 20 %, research about the stability is still retarded compared to commercialized OLEDs. It is common to see that the working lifetime of PeLEDs device is under an hour.[64-67] On the other hand, commercialized OLEDs can be maintained up to 100,000 hours and conventional QLEDs can be maintained up to 1000 hours. Therefore, to commercialize PeLEDs, the most important obstacle is solving its stability problem. In case of PeLEDs, ion migration, electrochemical reaction, and interfacial reaction are the problem and strong ionic character of perovskite and low formation energy are the origins of its instability.

For PeLEDs with those outstanding properties, excellent quality of perovskite solution should be prior to all. The quality of perovskite solution is directly related to its photoluminescence quantum yield (PLQY) which means the ratio of the number of photons emitted to the number of photons absorbed. PLQY defines the emission characteristic of perovskite solution, therefore, it affects to EQE of LEDs device also. To enhance PLQY, various method such as ligand engineering, modifying washing process, doping, and substitution have been tried.[68-70] Perovskite solution developed by those method can be confirmed by PLQY measurement or transmission electron microscopy (TEM). Especially with TEM, the size distribution of perovskite crystals can be confirmed, and one can see whether perovskite crystals are formed well or not.

Chapter 3
Perovskite Nanocrystals Light-Emitting Diodes Device with DIO Additive to Poly-TPD Layer

3.1 Research Background

As time goes by, producing energy is getting more important since the energy source is limited. At the same time, the way consuming the energy efficiently is also in the spotlight. Among the spots of energy consuming, light is one of the most frequently used energy, therefore, research about LEDs device employing various materials has been widely studied. Meanwhile, perovskite came into the spotlight due to its proper properties as mentioned in previous chapters. There are several class of perovskite which are classified by its dimension. To overcome the shortcoming of perovskite such as low exciton binding energy, making the dimension of perovskite low became one of the method to confine charge carriers into the perovskite crystals. Consequently, LEDs based on PeNCs became the hot topic of the optoelectronic device, and I decided to make highly efficient LEDs device based on PeNCs.

In this study, EQE of PeNCs LEDs were enhanced by manipulating interlayer with additive. The additive engineering was inspired by solar cell research. For example, DIO is used as an additive to active layer which is bulk heterojunction (BHJ) of PCPDTBT/$PC_{71}BM$.[71] For the first, DIO has selective solubility of the fullerene component, and second, DIO has higher boiling point than the host solvent which is CB. Due to these properties of DIO, DIO prevented $PC_{71}BM$ to be aggregated or stacked, and leads to better controlled morphology. Inspired by this result, DIO was introduced to the interlayer which is poly-TPD used as HTL in LEDs device, as shown in **Figure 3.1**. By adding DIO to poly-TPD, increased efficiency, enhanced morphology, and balanced charge injection between hole and electron were aimed.

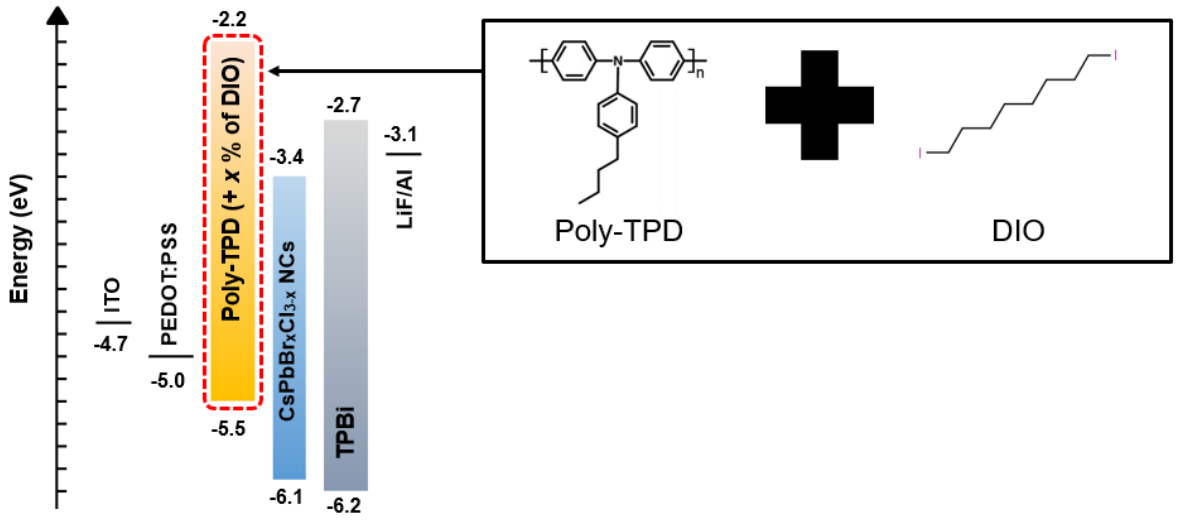

Figure 3.1 Overall scheme which introduces DIO additive into the poly-TPD layer and the device structure including respective bandgap of each layer.

3.2 Experimental Method & Materials

Materials

Cs_2CO_3 (Sigma-Aldrich, ReagentPlus, 99 %), PbBr2 (Alfa Aesar, metals basis, 99.999 %), DDAC (TCI, 98%), Ethyl acetate (Sigma-Aldrich), Octanoic acid (TCI), Toluene (Sigma-Aldrich, anhydrous, 99.8 %), TOAB (Sigma-Aldrich), Chlorobenzene (Sigma-Aldrich, anhydrous, 99.8 %), Hexane (Sigma-Aldrich, anhydrous, 95 %), TPBi (OSM, 99.9 %).

Synthesis of $CsPbBr_xCl_{3-x}$ PeNCs.

The synthesis of PeNCs solution was by LARP method. For the preparation of cesium oleate solution, 0.1 mmol of cesium carbonate (Cs_2CO_3) was loaded into a 100 mL three-neck flask along with 1 mL octanoic acid, then mixed by magnetic stirring. Next, 0.1 mmol of $PbBr_2$, 0.2 mmol of tetraoctylammonium bromide (TOAB) was dissolved in 1ml of toluene into a 50 mL three-neck flask. Then, 0.1 mL of cesium oleate solution was added to the $PbBr_2$ precursor solution. After that, 1ml of didodecyl dimethyl ammonium chloride (DDAC) of 30 $mgmL^{-1}$ in CB was added to the precursor solution. Then, for the purification step, the crude solution with ethyl acetate (volume ratio of crude/washing solvent 2:1) centrifuged at 12000 rpm for 5 min followed by one more centrifuge at 10000 rpm for 5 min. After that, precipitate which was dissolved in 1ml of hexane was centrifuged at 4000 rpm for 5 min, and the supernatant solution was collected. This was filtered also.

Preparation of poly-TPD solution with DIO as an additive

The concentration of poly-TPD in CB was 8 mg mL^{-1}. DIO additive was treated to the poly-TPD solution, and the volume fraction of DIO was varied as 0 %, 1 %, 3 %, 5 %, and 10 %. Prepared poly-TPD solution had been stored at the hot plate with 60 °C for a day.

Device Fabrication

ITO-patterned glass substrates were cleaned in deionized water, acetone, and IPA sequentially by using ultrasonication and it was dried in hot oven. Those ITO substrates went under UV ozone treatment to make the surface hydrophilic, and PEDOT:PSS solution was spin coated onto the UV ozone-treated ITO substrates at 3000rpm for 40s followed by annealing at 150 °C for 15 min. After the film was cooled down, the poly-TPD of 8 $mgmL^{-1}$ in chlorobenzene was spin coated at 2000 rpm for 60 s followed by annealing at 140 °C for 20 min in a N_2-filled glove box. Then, PeNCs layer were spin coated at 4000 rpm for 60 s. Finally, TPBi (50 nm), lithium fluoride (LiF) (1 nm), and aluminium (Al) (100 nm) were thermally evaporated sequentially under high vacuum ($<10^{-6}$ Torr). The active area of the device is 13.5 mm^2.

Photoluminescence Measurements

The photoluminescence spectra were measured with an nF900 instrument (Edinburgh Photonics) with a xenon lamp for the excitation source.

Time-Correlated Single-Photon Counting (TCSPC)

The PeNCs films was spin coated onto poly-TPD layer with the different quantity of DIO. The TCSPC setup (FluoTime 300) was used to measure the PL lifetime and the ratio of non-radiative recombination to radiative recombination. The samples were photoexcited with a 470 nm of continuous wave and pulsed diode laser head (LEHD-C-375). The time-integrated PL spectra were measured using a TCSPC module (PicoHarp) with a photomultiplier tube (PMA-C 182-N-M). The PL decay curves were fitted to a biexponential decay model (FluoFit).

AFM measurement

The surface morphology was scanned using an atomic force microscope (AFM) of VEECO Dimension 3100 equipped with Nanoscope V

Device Measurement

The J−V−L characteristics of LED devices were measured by using a Keithley 2400 source measurement unit and a Konica Minolta spectroradiometer (CS-2000).

3.3 Result & Discussion

To see optical property when DIO is added to poly-TPD layer, PL measurement was carried out by fluorometer. The measurement was according to the different volume percent of DIO to poly-TPD solution. **Figure 3.2** and **Figure 3.3** are PL result of thin film which structure is glass/poly-TPD (+ x % of DIO), and the difference is the thickness of PeNCs layer. If the PeNCs layer is coated thinly, double peak of PL is observed since photon emission is shown from both poly-TPD layer and PeNCs layer. By using this phenomenon, PeNCs were coated thinly in **Figure 3.2**, and change of PL intensity of poly-TPD and PeNCs were observed. As expected, relative PL intensity of poly-TPD is decreased when DIO is added. Then, when PeNCs were coated thickly compared to the previous condition, only single peak from PeNCs were observed. It means most of charge recombination appeared at PeNCs layer. Similarly, relative PL intensity was increased when DIO additive was used. In sight of this, DIO additive seems to affect to charge recombination mechanism between poly-TPD and PeNCs layer. This is because DIO participated in a role of interface passivation between poly-TPD and PeNCs layer. DIO passivated interface trap and reduced non-radiative recombination at the interface. Since DIO additive showed enhanced optical property, the further study was needed.

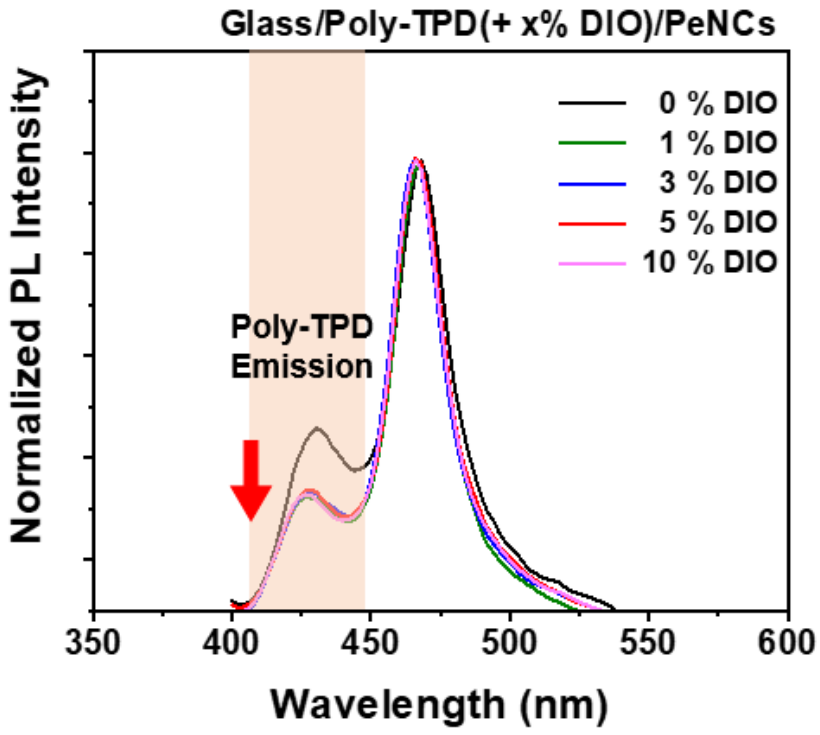

Figure 3.2 Normalized PL intensity of deposited perovskite nanocrystals with thin thickness on Glass/Poly-TPD (+ x % DIO) according to the different volume fraction of DIO.

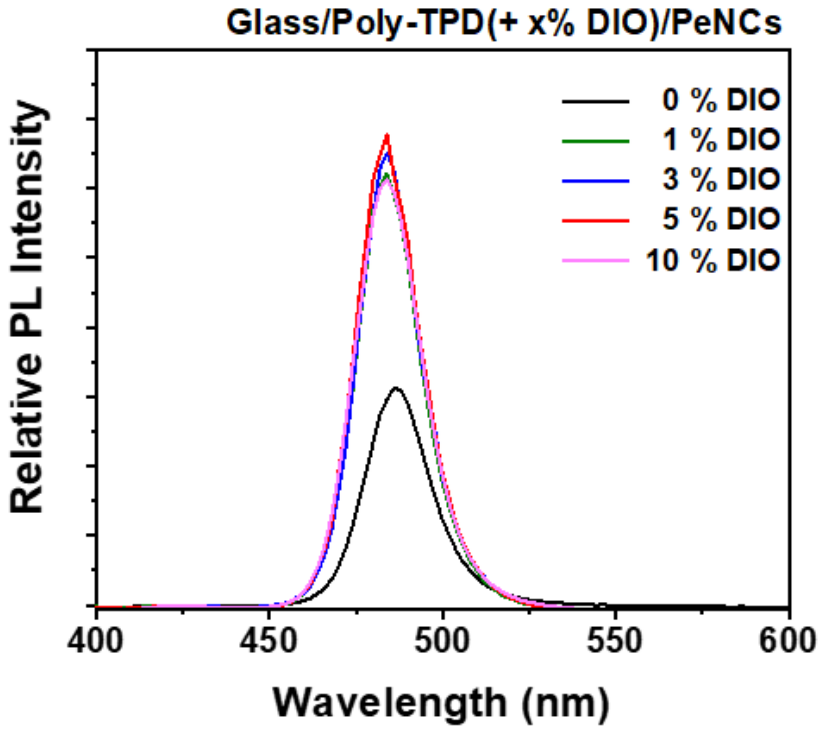

Figure 3.3 Relative PL intensity of deposited perovskite nanocrystals on Glass/Poly-TPD (+ x % DIO) according to different volume fraction of DIO.

Based on the PL measurement result, TCSPC measurement was also executed to confirm the effect of DIO on radiative recombination mechanism. PL lifetime and the ratio of non-radiative recombination to radiative recombination were measured according to the different volume percent of DIO to poly-TPD solution, as shown in **Figure 3.4**. The decay was designed to be fitted to the biexponential graph. The fast decay (τ_1) and slow decay (τ_2) are related to non-radiative and radiative recombination, respectively. Its lifetime and the proportion are shown in **Table 3.1**. Also, the average PL lifetime is calculated on the **Table 3.1**.

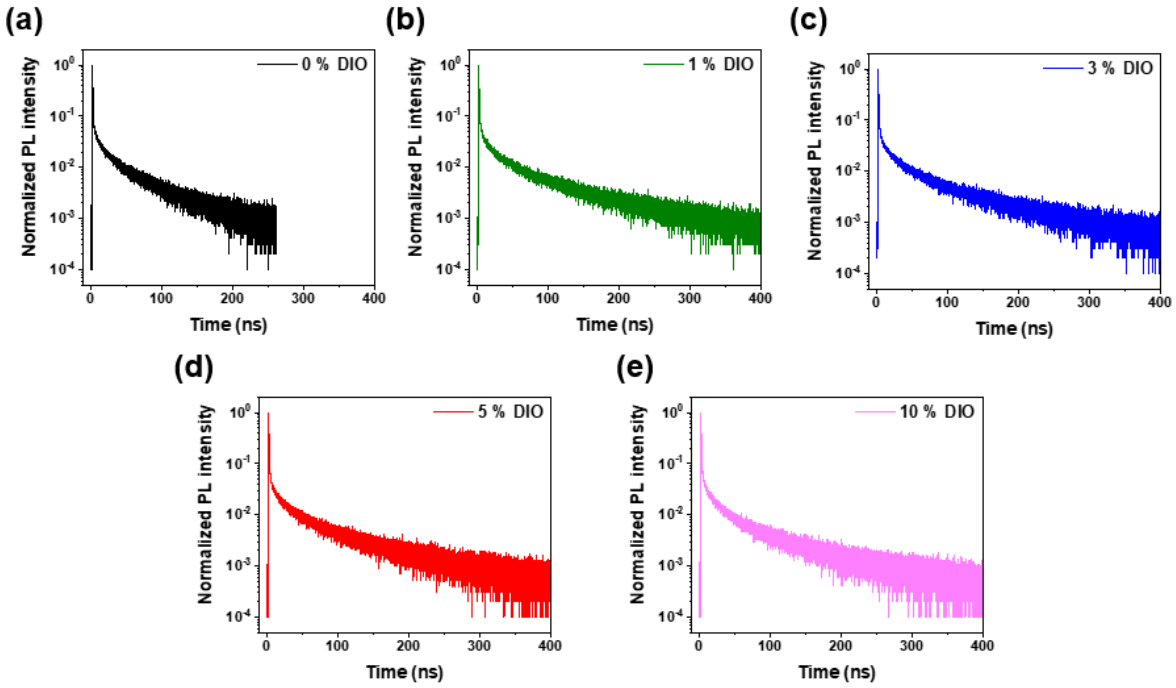

Figure 3.4 TCSPC of deposited perovskite nanocrystals with thin thickness on Glass/Poly-TPD (+ x % DIO) according to the different volume fraction of DIO; (a) 0 %, (b) 1 %, (c) 3 %, (d) 5 %, and (e) 10 % DIO additive to poly-TPD solution.

DIO	τ_1 (ns)	f_1 (%)	τ_2 (ns)	f_2 (%)	τ_{ave} (ns)	χ^2
0 %	1.54	79.46	35.28	20.54	8.47	1.81
1 %	3.36	78.40	58.02	21.60	15.17	1.75
3 %	5.16	75.97	65.98	24.03	19.78	1.51
5 %	5.78	75.06	66.87	24.94	21.01	1.38
10 %	5.85	75.29	59.20	24.71	19.03	1.37

Table 3.1 Biexponential fitting parameters for TCSPC of the perovskite film deposited on Glass/Poly-TPD (+ x % DIO) according to the different volume fraction ; f_1 and f_2 are percent contributions of lifetimes, fast-decay τ_1 and slow-decay τ_2, respectively.

PL lifetime of the PeNCs was remarkably increased near 3 times when DIO additive was used compared to the untreated film. When untreated, PL lifetime was only 8.47 ns, otherwise, when 5 % of DIO treated, PL lifetime was enhanced to 21.01 ns. It is caused by decreased contribution of non-radiative recombination. f_1 was gradually decreased from 79.46 % to 75.06 % when the condition was varied from 0 % to 5 % of DIO treated. Here, decreased contribution of non-radiative recombination indicates that DIO passivated the interface between poly-TPD and PeNCs layer. At the same time, extremely increased slow decay time can lead promising EQE of LEDs device. Also, This TCSPC result well matches with previous PL measurement data.

After the enhancement of the optical property confirmed, analysis on electrical property was also explored. For the first time, it was simply confirmed by measuring *I-V* characteristics of simple device which structure is ITO/Poly-TPD (+ x % of DIO)/Ag, as shown in **Figure 3.5**. The current injection was obviously increased. If the enhancement of current injection is also applied to the LEDs device, DIO has a good influence on the charge balance. Since the mobility of hole side is generally retarded compared to electron side due to compositive reason of mobility and injection barrier, which is come from the bandgap of materials, enhancement of hole side injection leads to better charge balance between both sides.[48]

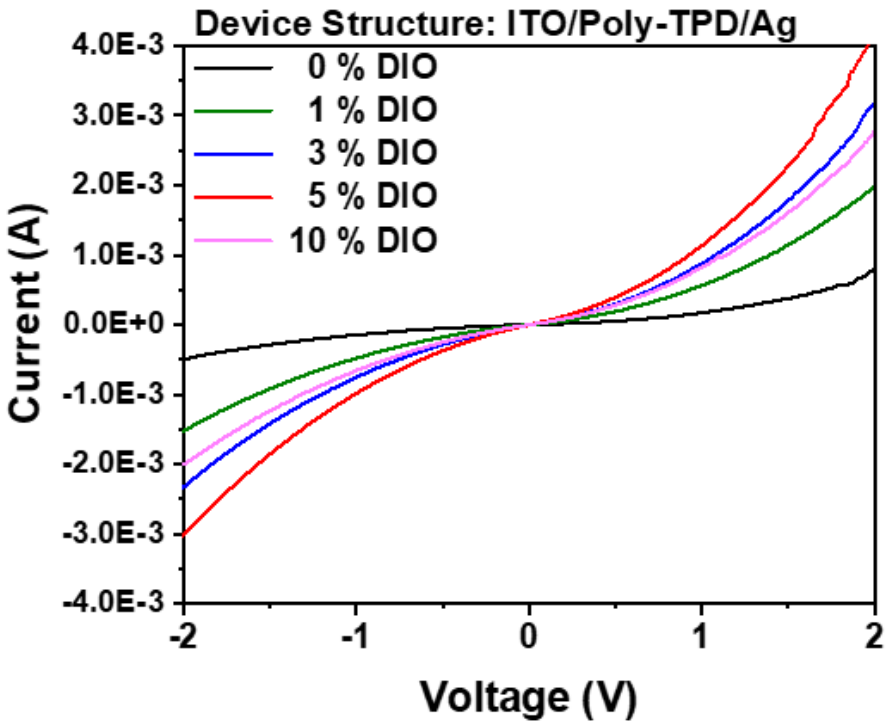

Figure 3.5 *I-V* characteristics of poly-TPD according to the different volume fraction of DIO; Device structure: ITO/Poly-TPD (+ x % of DIO)/Ag.

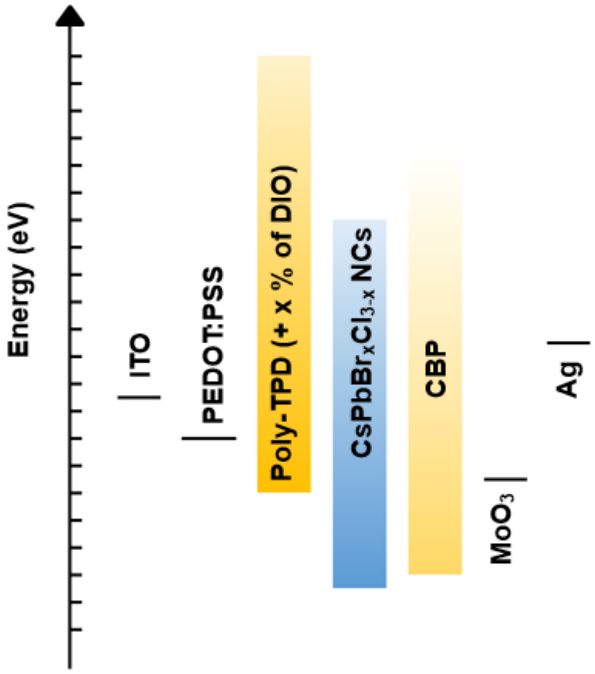

Figure 3.6 The structure of hole-only device and its respective bandgap of each layer; Device structure: ITO/PEDOT:PSS/Poly-TPD (+ x % of DIO)/PeNCs/CBP/MoO_3/Ag

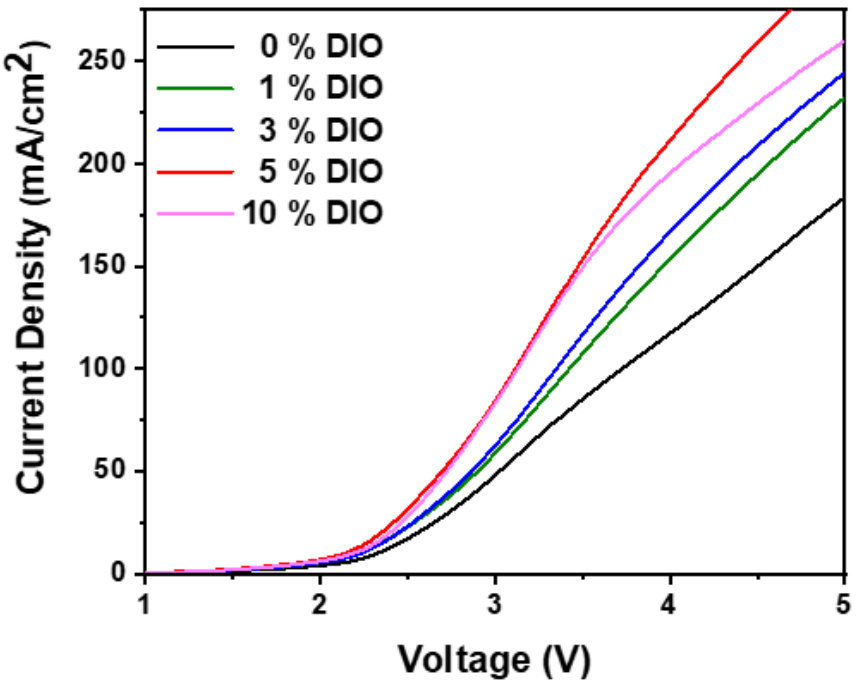

Figure 3.7 *J-V* characteristics of hole-only device which structure is ITO/PEDOT:PSS/Poly-TPD (+ x % of DIO)/CBP/MoO_3/Ag according to the different volume fraction of DIO.

Based on *I-V* result, hole-only device was fabricated to check charge injection characteristic of hole side according to the different quantity of DIO. The structure of the device was ITO/PEDOT:PSS/Poly-TPD (+ x % of DIO)/PeNCs/CBP/MoO3/Ag, as shown in **Figure 3.6**, and *J-V* characteristic was shown in **Figure 3.7**. The result of *J-V* characteristic had the same tendency with the previous *I-V* measurement, and the current injection was to the maximum when 5 % of DIO was added.

To investigate the reason of these enhancement of current injection, hole mobility of poly-TPD layer was calculated by fitting SCLC flow, as shown in **Figure 3.8**. Since the hole mobility of untreated poly-TPD was calculated as 7×10^{-5} which is similar with the reported reference hole mobility of poly-TPD which is 1×10^{-4}, reliability of the data is ensured. The mobility of poly-TPD was to the maximum when 5 % of DIO was treated, and the mobility was 1.4×10^{-4}. Based on this, the fact that the enhancement of mobility of poly-TPD affected to the increasement of charge injection was proved.

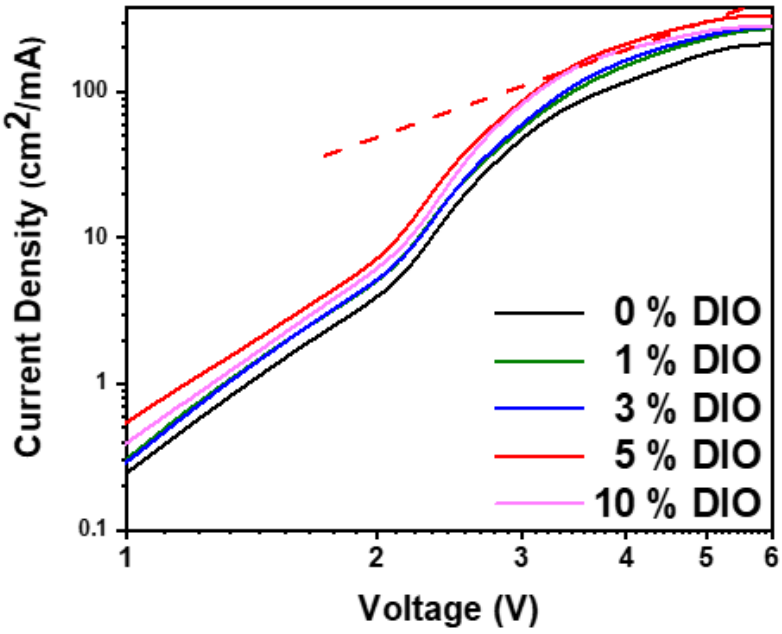

Figure 3.8 J-V characteristics of poly-TPD according to the different volume fraction of DIO and SCLC fitted.

	0 %	1 %	3 %	5 %	10 %
Mobility [cm²/V·S]	7 x 10^{-5}	9 x 10^{-5}	1 x 10^{-4}	1.4 x 10^{-4}	1.2 x 10^{-4}

Table 3.2 The calculated hole mobility of poly-TPD layer according to the different volume fraction of DIO

Also, to explore the reason of enhanced contribution of radiative recombination and current injection, atomic force microscopy (AFM) measurement was carried out. The topographical image of AFM measurement was shown in **Figure 3.9**. The structure of the film was Glass/PEDOT:PSS/Poly-TPD (+ x % of DIO). As shown in the figure, morphology of the film was enhanced by adding DIO. Compared to the reference which has 0.634nm of root-mean-square (Rq), Rq was decreased to 0.391 nm when 5 % of DIO was added. In addition, there are aggregates on the poly-TPD film in 0 % condition, otherwise, DIO-treated film showed clear film images without the aggregates. With the AFM results, morphology and roughness of the thin film was highly improved by adding DIO to poly-TPD layer. It is regarded that this affected to the enhanced radiative recombination and hole injection.

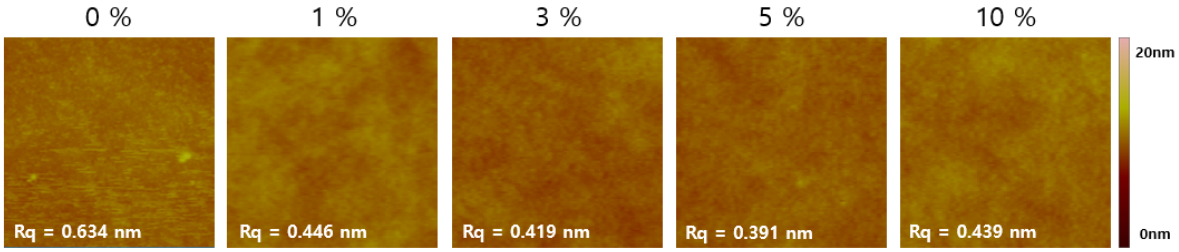

Figure 3.9 AFM topographical images of Glass/PEDOT:PSS/Poly-TPD (+ x % DIO) according to the different volume fraction of DIO; (a) 0 %, (b) 1 %, (c) 3 %, (d) 5 %, and (e) 10 %.

Likewise, the role of DIO additive can be explained in two main ways. One is the enhancement of optical property by passivating trap sites at the interface, and the other is the improvement of hole injection caused by increased hole mobility of poly-TPD layer.

Based on this, EL device was fabricated with the structure of ITO/PEDOT:PSS/Poly-TPD (+ x % of DIO)/PeNCs/TPBi/LiF/Al. The green LEDs are fabricated with $CsPbBr_3$, and the blue LEDs were fabricated with $CsPbBr_xCl_{3-x}$. The EL emission by PeNCs which were CsPbBr3 was observed at 514 nm, as shown in **Figure 3.10**b. To optimize the performance of the EL device, the quantity of DIO additive was varied from 0 % to 10 %. The optimized performance of the EL device is shown in **Figure 3.10** and **Table 3.3**. The highest EQE was observed with 5 % of DIO treated condition. It was 5.17 % which was almost doubled compared to the pristine device. Also, CE showed the same tendency with EQE, and it was increased from 9.52 cd A^{-1} to 17.05 cd A^{-1} when the volume fraction of DIO was changed from 0 % to 5 %. The EL emission by PeNCs which is $CsPbBr_xCl_{3-x}$ was observed at 476 nm, as shown in **Figure 3.11**b. Also, very narrow FWHM around 16nm which is one of the outstanding property of perovskite was observed. To optimize the performance of the EL device, the quantity of DIO additive was varied from 0 % to 10 %. The optimized performance of the EL device was shown in **Figure 3.11** and **Table 3.4**. The highest EQE was observed with 5 % of DIO treated condition. It was 1.34 % which was almost 3 times as much as 0.58 % which was from DIO untreated condition. Also,

CE showed the same tendency with EQE, and it was increased from 0.76 cd A^{-1} to 1.85 cd A^{-1} when the volume fraction of DIO was changed from 0 % to 5 %. This enhancement of efficiency is directly related to PL lifetime and hole mobility data. Moreover, turn-on voltage of the EL device was decreased when DIO was treated. Here, the turn-on voltage is defined as the voltage when the luminance of the EL device shows is 1 cd m^{-2}. The turn-on voltage of the reference device was 5 V, but it was decreased when DIO was treated. It showed 3.75 V when 5 % of DIO was added. This is caused by the enhancement of the charge injection and improved charge balance. In addition, the enhancement of turn-on voltage was more remarkable for blue device than green one because blue active layer which has larger bandgap is more affected by hole injection. Also, the current density before the turn-on indicates leakage current of the device. All the devices regardless of the quantity of DIO showed very low leakage current as shown in **Figure 3.10**a and **Figure 3.11**a, and especially when 3 % or 5 % of DIO was added, extremely low leakage current was measured. It is directly related to the enhanced film morphology of poly-TPD layer.

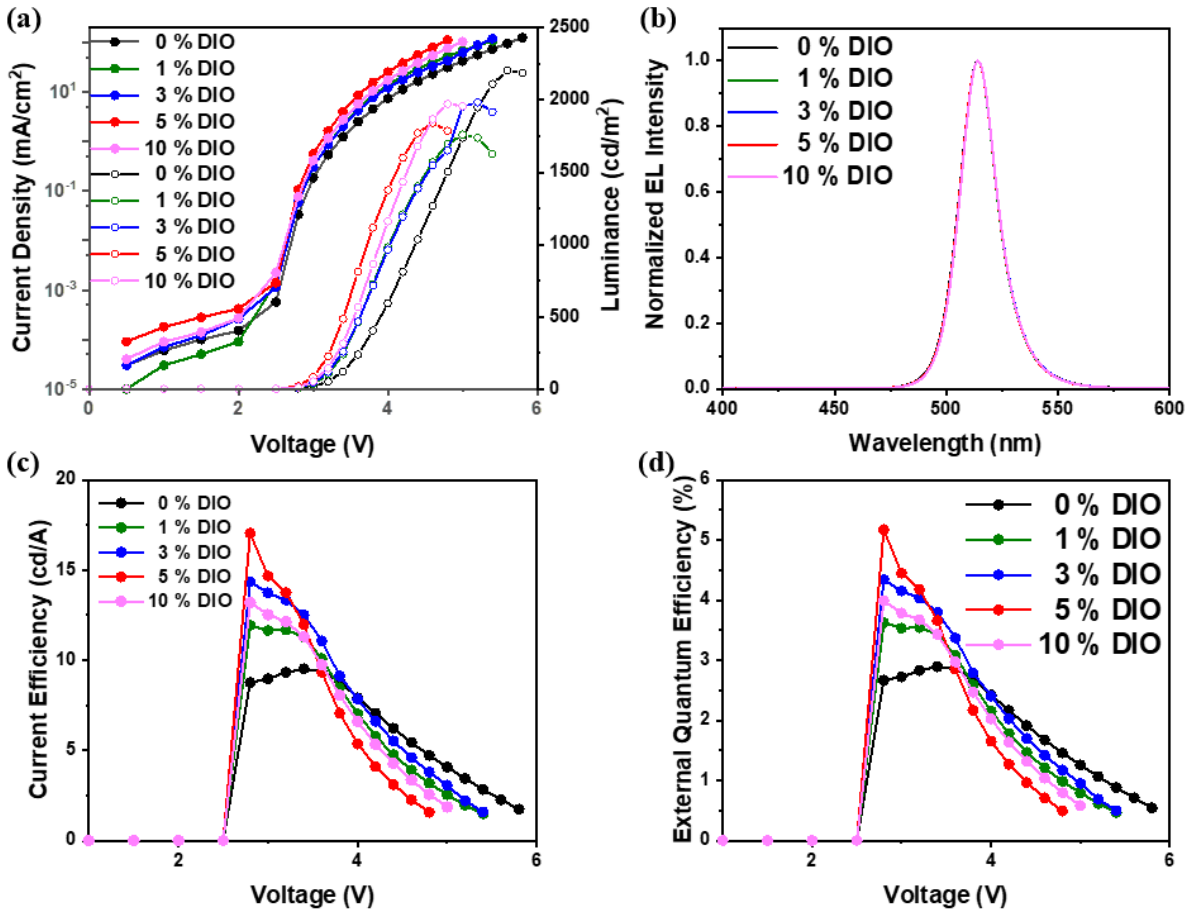

Figure 3.10 The performance of green EL device according to the different volume fraction of DIO to poly-TPD solution; (a) *J-V-L* characteristic, (b) normalized EL intensity, (c) CE, (d) EQE.

DIO vol% in poly-TPD solution [%]	Maximum Luminance [cd/m²] [at voltage]	Maximum Current Efficiency [cd/A] [at voltage]	EQE [%] [at voltage]	FWHM [nm]
0	2203.6@5.6V	9.52@3.4V	2.89@3.4V	20.07
1	1760.1@5.0V	11.94@2.8V	3.62@2.8V	19.61
3	1983.7@5.2V	14.35@2.8V	4.34@2.8V	20.07
5	1842.4@4.6V	17.05@2.8V	5.17@2.8V	20.07
10	1973.0@4.8V	13.20@2.8V	3.99@2.8V	19.84

Table 3.3 The performance of green EL device including maximum luminance, maximum CE, EQE, and FWHM according to the different volume fraction of DIO to poly-TPD solution

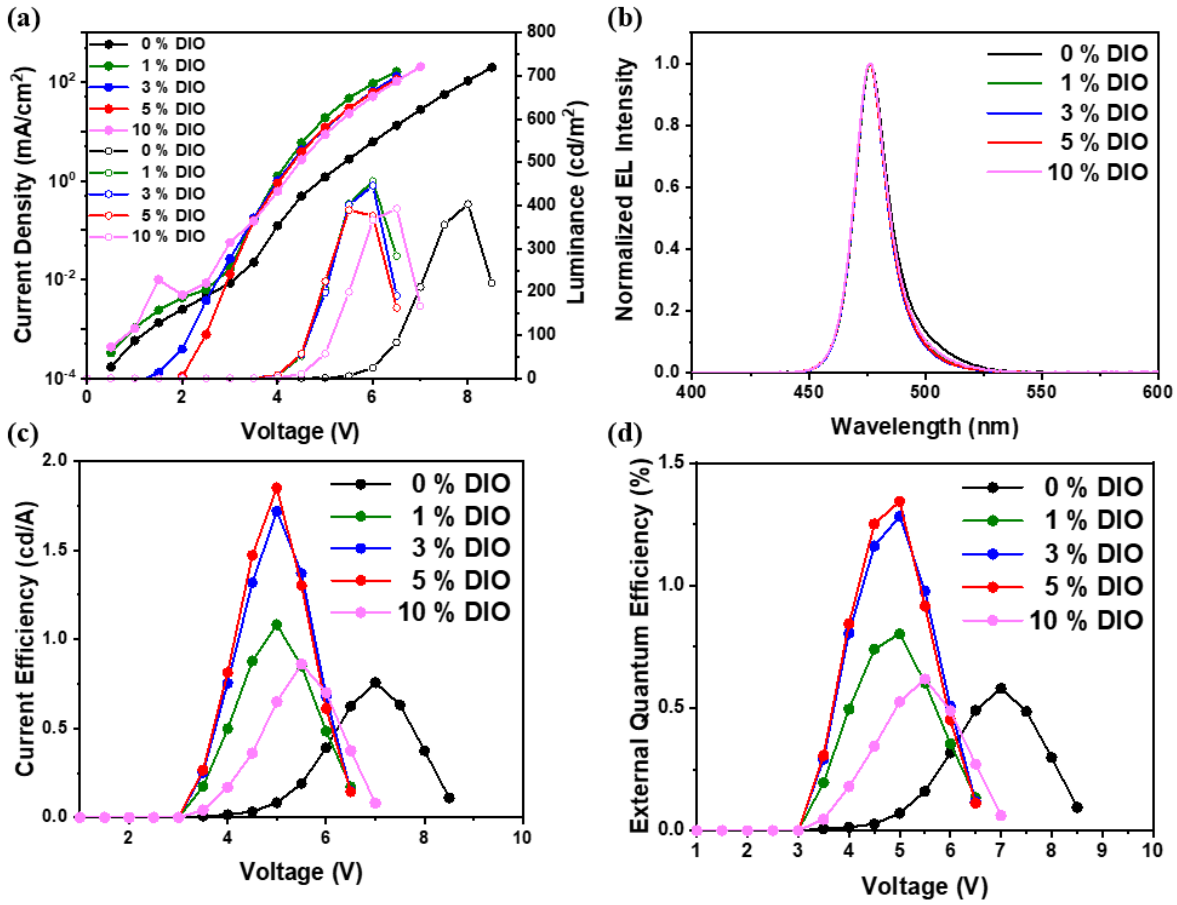

Figure 3.11 The performance of blue EL device according to the different volume fraction of DIO to poly-TPD solution; (a) *J-V-L* characteristic, (b) normalized EL intensity, (c) CE, (d) EQE.

DIO vol% in poly-TPD solution [%]	Maximum Luminance [cd/m^2] [at voltage]	Maximum Current Efficiency [cd/A] [at voltage]	EQE [%] [at voltage]	FWHM [nm]	Turn-on Voltage [V]
0	403.46@8.0V	0.76@7.0V	0.58@7.0V	20.00	5
1	456.79@6.0V	1.08@5.0V	0.80@5.0V	16.28	3.75
3	446.21@6.0V	1.72@5.0V	1.28@5.0V	16.03	3.75
5	390.00@5.5V	1.85@5.0V	1.34@5.0V	16.27	3.75
10	393.18@6.5V	0.86@5.5V	0.62@5.5V	16.63	4

Table 3.4 The performance of EL device including maximum luminance, maximum CE, EQE, FWHM, and turn-on voltage according to the different volume fraction of DIO to poly-TPD solution

3.4 Conclusion

In summary, the PeNCs LEDs device with poly-TPD treated by DIO additive was successful fabricated and effect of DIO was confirmed. Clear green emission regions at 514 nm, blue emission region at 476 nm, and very narrow FWHM were measured. Since the blue PeNCs LEDs device have been a problem due to its low EQE, especially enhancement of blue LEDs EQE was the big achievement.

By using DIO additive, the role of DIO additive can be explained in two main ways; (a) one is the enhancement of optical property by passivating trap sites at the interface, and (b) the other is the improvement of hole injection caused by increased hole mobility of poly-TPD layer. The enhancement of optical property was confirmed by PL and TCSPC measurement. Also, the improvement of hole injection was confirmed by hole-only device and fitting SCLC. This is regarded as the result of enhanced morphology of thin film and decreased roughness which were confirmed by AFM measurement. Furthermore, green and blue PeNCs LEDs device were fabricated and it showed highly enhanced EQE from 2.89 % from 5.17 % and from 0.58 % to 1.34 %, respectively. Also, earlier turn-on was observed when DIO was treated on both colors. It means that charge balance was improved, and electrical property of the device was reinforced. In addition, this study will suggest one of the way to increase the efficiency of PeNCs LEDs device.

REFERENCE

1. Burroughes, J. H.; Bradley, D. D. C.; Brown, A. R.; Marks, R. N.; MacKay, K.; Friend, R. H.; Burns, P. L.; Holmes, A. B. "Light-emitting diodes based on conjugated polymers". *Nature* **1990**, 347 (6293), 539–541
2. Saleh, B. E. A.; Teich, M. C. "Fundamentals of photonics", *Wiley Interscience* **2007**
3. Holonyak Nick; Bevacqua, S. F. "Coherent (Visible) Light Emission from Ga($As_{1-x}P_x$) Junctions". *Applied Physics Letters* **1962**, 1 (4), 82
4. Tang, C. W.; Van Slyke, S. A. "Organic electroluminescent diodes". *Applied Physics Letters* **1987**, 51 (12), 913
5. Baldo, M. A.; Lamansky, S.; Burrows, P. E.; Thompson, E.; and Forrest. S. R. "Very high-efficiency green organic light-emitting devices based on electrophosphorescence". *Applied Physics Letters* **1999**, 75 (1), 4
6. Tan, Z. K.; Moghaddam, R. S.; Lai, M. L.; Docampo, P.; Higler, R.; Deschler, F.; Price, M.; Sadhanala, A.; Pazos, L. M.; Credgington, D. "Bright Light-Emitting Diodes Based on Organometal Halide Perovskite". *Nature Nanotechnology* **2014**, 9, 687–692
7. Cho, H; Jeong, S. H.; Park, M. H.; Kim, Y. H.; Wolf, C.; Lee, C. L.; Heo, J. H.; Sadhanala, A.; Myoung, N.; Yoo, S.; Im, S. H.; Friend, R. H.; Lee, T. W.; "Overcoming the electroluminescence efficiency limitations of perovskite light-emitting diodes". *Science* **2015**, 350 (6265), 1222-1225
8. Yu, J. C.; Kim, D. B.; Jung, E. D.; Lee, B. R.; Song, M. H. "High-performance perovskite light-emitting diodes s morphological control of perovskite films". *Nanoscale* **2016**, 8 (13), 7036-7042
9. Mitzi, D. B.; Feild, C. A.; Harrison, W. T. A.; Guloy, A. M. "Conducting tin halides with a layered organic-based perovskite structure". *Nature* **1994**, 369, 467–469
10. Era, M.; Morimoto, S.; Tsutsui, T.; Saito, S. "Organic-inorganic heterostructure electroluminescent device using a layered perovskite semiconductor $(C_6H_5C_2H_4NH_3)_2PbI_4$" *Applied Physics Letter*s **1994**, 65, 676
11. Yuan, M.; Quan, L. N.; Comin, R.; Walters, G.; Sabatini, R.; Voznyy, O.; Hoogland, S.; Zhao, Y.; Beauregard, E. M.; Kanjanaboos, P.; Lu, Z.; Kim, D. H.; Sargent, E. H.; "Perovskite energy funnels for efficient light-emitting diodes". *Nature Nanotechnology* **2016**, 11, 872–877
12. Ban, M.; Zou, Y.; Rivett, P. H.; Yang, Y.; Thomas, T. H.; Tan, Y.; Song, T.; Gao, X.; Credgington, D.; Deschler, F.; Sirringhaus, H.; Sun, B. "Solution-processed perovskite light emitting diodes with efficiency exceeding 15% through additive-controlled nanostructure tailoring". *Nature Communications* **2018**, 9, 3892
13. Kojima, A.; Ikegami, M.; Teshima, K.; Miyasaka, T. "Highly Luminescent Lead Bromide Perovskite Nanoparticles Synthesized with Porous Alumina Media". *Chemistry Letters* **2012**, 41

(4), 397-399

14. Protesescu, L.; Yakunin, S.; Bodnarchuk, M. I.; Krieg, F.; Caputo, R.; Hendon, C. H.; Yang, R. X.; Walsh, A.; Kovalenko, M. V. "Nanocrystals of Cesium Lead Halide Perovskites ($CsPbX_3$, X = Cl, Br, and I): Novel Optoelectronic Materials Showing Bright Emission with Wide Color Gamut". *Nano Letters* **2015**, 15 (6), 3692–3696
15. Zhang, F.; Zhong, H.; Chen, C.; Wu, X. G.; Hu, X.; Huang, H.; Han, J.; Zou, B.; Dong, Y. "Brightly Luminescent and Color-Tunable Colloidal $CH_3NH_3PbX_3$ (X = Br, I, Cl) Quantum Dots: Potential Alternatives for Display Technology". *ACS Nano* **2015**, 9 (4), 4533–4542
16. Song, J.; Li, J.; Li, X.; Xu, L.; Dong, Y.; Zeng, H. "Quantum Dot Light-Emitting Diodes Based on Inorganic Perovskite Cesium Lead Halides ($CsPbX_3$)". *Advanced Materials* **2015**, 27 (44), 7162-7167
17. Song, J.; Fang, T.; Li, J.; Xu, L.; Zhang, F.; Han, B.; Shan, Q.; Zeng, H. "Organic–Inorganic Hybrid Passivation Enables Perovskite QLEDs with an EQE of 16.48%". *Advanced Materials* **2018**, 30 (50), 1805409
18. Goldschmidt. V. M. "Die Gesetze der Krystallochemie". *The Science of Nature* **1926**, 14, 477–485
19. Eperon, G. E.; Stranks, S. D.; Menelaou, C.; Johnston, M. B.; Herza, L. M.; Snaith, H. J. "Formamidinium lead trihalide: a broadly tunable perovskite for efficient planar heterojunction solar cells". *Energy & Environmental Science* **2014**, **7** (3), 982-988
20. Pang, S.; Hu, H.; Zhang, J.; Lv, S.; Yu, Y.; Wei, F.; Qin, T.; Xu, H.; Liu, Z.; Cui, G. "NH2CH═NH2PbI3: An Alternative Organolead Iodide Perovskite Sensitizer for Mesoscopic Solar Cells". *Chemistry of Materials* **2014**, 26 (3), 1485–1491
21. Burschka, J.; Pellet, N.; Moon, S.-J.; Humphry-Baker, R.; Gao, P.; Nazeeruddin, M. K.; Grätzel, M. "Sequential deposition as a route to high-performance perovskite-sensitized solar cells". *Nature* **2013**, 499, 316–319
22. Koh, T. M.; Fu, K.; Fang, Y.; Chen, S.; Sum, T.; Mathews, N.; Mhaisalkar, S. G.; Boix, P. P.; Baikie, T. "Formamidinium-Containing Metal-Halide: An Alternative Material for Near-IR Absorption Perovskite Solar Cells". *The Journal of Physical Chemistry C* **2013**, 118 (30), 16458–16462
23. Li, N.; Song, L.; Jia, Y.; Dong, Y.; Xie, F.; Wang, L.; Tao, S.; Zhao, N. "Stabilizing Perovskite Light-Emitting Diodes by Incorporation of Binary Alkali Cations". *Advanced Materials* **2020**, 32 (17), 1907786
24. Cho, H.; Kim, J. S.; Wolf, C.; Kim, Y.-H.; Yun, H. J.; Jeong, S.-H.; Sadhanala, A.; Venugopalan, V.; Choi, J. W.; Lee, C.-L.; Friend, R. H.; Lee. T.-W. "High-Efficiency Polycrystalline Perovskite Light-Emitting Diodes Based on Mixed Cations". *ACS Nano* **2018**, 12 (3), 2883–2892
25. Jeon, N. J.; Noh, J. H.; Yang, W. S.; Kim, Y. C.; Ryu, S.; Seo. J; Seok. S. I. "Compositional engineering of perovskite materials for high-performance solar cells". *Nature* **2015**, 517, 476–480
26. Song, J.; Li, J.; Xu, L.; Li, J.; Zhang, F.; Han, B.; Shan, Q.; Zeng, H. "Room-Temperature Triple-

Ligand Surface Engineering Synergistically Boosts Ink Stability, Recombination Dynamics, and Charge Injection toward EQE-11.6% Perovskite QLEDs". *Advanced Materials* **2018**, 30 (30), 1800764

27. Stoumps, C. C.; Malliakas, C. D.; Kanatzidis, M. G. "Semiconducting tin and lead iodide perovskites with organic cations: phase transitions, high mobilities, and near-infrared photoluminescent properties". *Inorganic Chemistry* **2013**, 52 (15), 9019–9038
28. Hao, F.; Stoumpos, C. C.; Cao, D. H.; Chang, R. P.; Kanatzidis, M. G. "Lead-free solid-state organic-inorganic halide perovskite solar cells". *Nature Photonics* **2014**, 8, 489–494
29. Bernal, C.; Yang, K. "First-Principles Hybrid Functional Study of the Organic–Inorganic Perovskites $CH_3NH_3SnBr_3$ and $CH_3NH_3SnI_3$". *The Journal of Physical Chemistry C* **2014**, 118 (42), 24383–24388
30. Umari, P.; Mosconi, E.; De Angelis, F. "Relativistic GW calculations on $CH_3NH_3PbI_3$ and $CH_3NH_3SnI_3$ Perovskites for Solar Cell Applications". *Scientific reports* **2014**, 4, 4467
31. Ogomi, Y.; Morita, A.; Tsukamoto, S.; Saitho, T.; Fujikawa, N.; Shen, Q.; Toyoda, T.; Yoshino, K.; Pandey, S. S.; Ma, T. "$CH_3NH_3Sn_xPb_{(1-x)}I_3$ Perovskite Solar Cells Covering up to 1060 nm". *The Journal of Physical Chemistry Letters* **2014**, 5 (6), 1004–1011
32. Lau, C. F. J.; Deng, X.; Zheng, J.; Kim, J.; Zhang, Z.; Zhang, M.; Bing, J.; Wilkinson, B.; Hu, L.; Patterson, R.; Huang, S.; Ho-Baillie, A. "Enhanced performance via partial lead replacement with calcium for a CsPbI3 perovskite solar cell exceeding 13% power conversion efficiency". *Journal of Materials Chemistry A* **2018**, 6 (14), 5580-5586
33. Ayatullahah, H.; Murtaza, G.; Muhammad, S.; Naeem, S.; Khalid, M. N.; Manzar, A. "Physical Properties of $CsSnM_3$ (M = Cl, Br, I): A First Principle Study". *Acta Physica Polonica A* **2013**, 124, 102
34. Kojima, A.; Teshima, K.; Shirai, Y.; Miyasaka, T. "Organometal Halide Perovskites as Visible-Light Sensitizers for Photovoltaic Cells". *Journal of the American Chemical Society* **2009**, 131 (17), 6050–6051
35. Im, J.-H.; Lee, C.-R.; Lee, J.-W.; Park, S.-W.; Park, N.-G. "6.5% efficient perovskite quantum-dot-sensitized solar cell". *Nanoscale* **2011**, 3 (10), 4088-4093
36. Mosconi, E.; Amat, A.; Nazeeruddin, M. K.; Grätzel, M.; De Angelis, F. "First-Principles Modeling of Mixed Halide Organometal Perovskites for Photovoltaic Applications". *The Journal of Physical Chemistry C* **2013**, 117 (27), 13902-13913
37. Jiang, M.; Wu, J.; Lan, F.; Tao, Q.; Gao, D.; Li, G. "Enhancing the performance of planar organo-lead halide perovskite solar cells by using a mixed halide source". *Journal of Materials Chemistry A* **2015**, 3 (3), 963-967
38. Sadhanala, A.; Ahmad, S.; Zhao, B.; Giesbrecht, N.; Pearce, P. M.; Deschler, F.; Hoye, R. L. Z.; Gödel, K. C.; Bein, T.; Docampo, P.; Dutton, S. E.; De Volder, M. F. L.; Friend, R. H. "Blue-Green

Color Tunable Solution Processable Organolead Chloride–Bromide Mixed Halide Perovskites for Optoelectronic Applications". *Nano Letters* **2015**, 15 (9), 6095-6101

39. Chiba, T.; Hayashi, Y.; Ebe, H.; Hoshi, K.; Sato, J.; Sato, S.; Pu, Y.-J.; Ohisa, S.; Kido, J. "Anion-exchange red perovskite quantum dots with ammonium iodine salts for highly efficient light-emitting devices". *Nature Photonics* **2018**, 12, 681-687
40. Knight, A. J.; Herz, L. M. "Preventing phase segregation in mixed-halide perovskites: a perspective". *Energy & Environmental Science* **2020**, 13 (7), 2024-2046
41. Yoon, Y. J.; Shin, Y. S.; Park, C. B.; Son, J. G.; Kim, J. W.; Kim, H. S.; Lee, W.; Heo, J.; Kim, G.-H.; Kim, J. Y. "Origin of Luminescence Spectra Width in Perovskite Nanocrystals with Surface Passivation". *Nanoscale* **2020**
42. Tang, C. W.; Van Slyke, S. A.; Chen, C. H. "Electroluminescence of doped organic thin films". *Journal of Applied Physics* **1989**, 65 (9), 3610
43. Adachi, C.; Baldo, M. A.; Thompson, M. E.; Forrest. S. R. "Nearly 100% internal phosphorescence efficiency in an organic light-emitting device". *Journal of Applied Physics* **2001**, 90 (10), 5048
44. Chang, Y.-L.; Wang, Z. B.; Helander, M. G.; Qiu, J.; Puzzo, D.P.; Lu, Z. H. "Enhancing the efficiency of simplified red phosphorescent organic light emitting diodes by exciton harvesting". *Organic Electronics* **2012**, 13 (5), 925-931
45. Zhang, Q.; Li, B.; Huang, S.; Nomura, H.; Tanaka, H.; Adachi, C. "Efficient blue organic light-emitting diodes employing thermally activated delayed fluorescence". *Nature Photonics* **2014**, 8, 326-332
46. Duan, L.; Hou, L.; Lee, T.-W.; Qiao, J.; Zhang, D.; Dong, G.; Wang, L.; and Qiu, Y. "Solution processable small molecules for organic light-emitting diodes". *Journal of Materials Chemistry* **2010**, 20, 6392-6407
47. Kim, Y.-H.; Cho, H.; Heo, J. H.; Kim, T.-S.; Myoung, N.; Lee, C.-L.; Im, S. H.; Lee, T.-W. "Multicolored Organic/Inorganic Hybrid Perovskite Light-Emitting Diodes". *Advanced Materials* **2015**, 27 (7), 1248-1254
48. Zou, Y.; Ban, M.; Yang, Y.; Bai, S.; Wu, C.; Han, Y.; Wu, T.; Tan, Y.; Huang, Q.; Gao, X.; Song, T.; Zhang, Q.; Sun, B. "Boosting Perovskite Light-Emitting Diode Performance via Tailoring Interfacial Contact". *ACS Applied Materials & Interfaces* **2018**, 10 (28), 24320–24326
49. Chih, Y.-K.; Wang, J.-C.; Yang, R.-T.; Liu, C.-C.; Chang, Y.-C.; Fu, Y.-S.; Lai, W.-C.; Chen, P.; Wen, T.-C.; Huang, Y.-C.; Tsao, C.-S.; Guo, T.-F. "NiO_x Electrode Interlayer and CH3NH2/CH3NH3PbBr3 Interface Treatment to Markedly Advance Hybrid Perovskite-Based Light-Emitting Diodes". *Advanced Materials* **2016**, 28 (39), 8687-8694
50. Hoye, R. L. Z.; Chua, M. R.; Musselman, K. P.; Li, G.; Lai, M.-L.; Tan, Z.-K.; Greenham, N. C.; MacManus-Driscoll, J. L.; Friend, R. H.; Credgington, D. "Enhanced Performance in Fluorene-Free Organometal Halide Perovskite Light-Emitting Diodes using Tunable, Low Electron Affinity

Oxide Electron Injectors". *Advanced Materials* **2015**, 27 (8), 1414-1419

51. Wang, J.; Wang, N.; Jin, Y.; Si, J.; Tan, Z.-K.; Du, H.; Cheng, L.; Dai, X.; Bai, S.; He, H.; Ye, Z.; Lai, M. L.; Friend, R. H.; Huang, W. "Interfacial Control Toward Efficient and Low-Voltage Perovskite Light-Emitting Diodes". *Advanced Materials* **2015**, 27 (14), 2311-2316
52. Simkus, G.; Sanders, S.; Stümmler, D.; Vescan, A.; Kalisch, H.; Heuken, M. "High-Intensity CsPbBr3 Perovskite LED using Poly(bis(4-phenyl)(2,4,6-trimethylphenyl)amine) as Hole Transport and Electron-Blocking Layer". *MRS Advances* **2020**, 5 (8-9), 411-419
53. Chen, H.; Ding, K.; Fan, L.; Liu, W.; Zhang, R.; Xiang, S.; Zhang, Q.; Wang, L. "All-Solution-Processed Quantum Dot Light Emitting Diodes Based on Double Hole Transport Layers by Hot Spin-Coating with Highly Efficient and Low Turn-On Voltage". *ACS Applied Materials & Interfaces* **2018**, 10 (34), 29076–29082
54. Araújoa, F. L.; Amorim, D. R. B.; Torres, B. B. M.; Coutinho, D. J.; Faria, R. M. "Effects of additive-solvents on the mobility and recombination of a solar cell based on PTB7-Th:PC71BM". *Solar Energy* **2019**, 177, 284-292
55. Turren-Cruz, S.-H.; Saliba, M.; Mayer, M. T.; Juárez-Santiesteban, H.; Mathew, X.; Nienhaus, L.; Tress, W.; Erodici, M. P.; Sher, M.-J.; Bawendi, M. G.; Grätzel, M.; Abate, A.; Hagfeldt, A.; Correa-Baena, J.-P. "Enhanced charge carrier mobility and lifetime suppress hysteresis and improve efficiency in planar perovskite solar cells". *Energy & Environmental Science* **2018**, 11 (1), 78-86
56. Stranks, S. D.; Hoye, R. L. Z.; Di, D.; Friend, R. H.; Deschler, F. "The Physics of Light Emission in Halide Perovskite Devices". *Advanced Materials* **2018**, 31 (47), 1803336
57. Shin, Y. S.; Yoon, Y. J.; Heo, J.; Song, S.; Kim, J. W.; Park, S. Y.; Cho, H. W.; Kim, G.-H.; Kim, J. Y. "Functionalized PFN-X (X = Cl, Br, or I) for Balanced Charge Carriers of Highly Efficient Blue Light-Emitting Diodes". *ACS Applied Materials & Interfaces* **2020**, 12 (31), 35740–35747
58. Zhang, L.; Yang, X.; Jiang, Q.; Wang, P.; Yin, Z.; Zhang, X.; Tan, H.; Yang, Y.; Wei, M.; Sutherland, B. R.; Sargent, E. H.; You, J. "Ultra-bright and highly efficient inorganic based perovskite light-emitting diodes". *Nature Communications* **2017**, 8, 15640
59. McMeekin, D. P.; Wang, Z.; Rehman, W.; Pulvirenti, F.; Patel, J. B.; Noel, N. K.; Johnston, M. B.; Marder, S. R.; Herz, L. M.; Snaith, H. J. "Crystallization Kinetics and Morphology Control of Formamidinium–Cesium Mixed-Cation Lead Mixed-Halide Perovskite via Tunability of the Colloidal Precursor Solution". *Advanced Materials* **2017**, 29 (29), 1607039
60. Yu, J. C.; Park, J. H.; Lee, S. Y.; Song, M. H. "Effect of perovskite film morphology on device performance of perovskite light-emitting diodes". *Nanoscale* **2019**, 11 (4), 1505-1514
61. Liang, J.; Zhang, Y.; Guo, X.; Gan, Z.; Lin, J.; Fana, Y.; Liu X. "Efficient perovskite light-emitting diodes by film annealing temperature control". *RSC Advances* **2016**, 6 (75), 71070-71075
62. Sun, Y.; Zhang, L.; Wang, N.; Zhang, S.; Cao, Y.; Miao, Y.; Xu, M.; Zhang, H.; Li, H.; Yi, C.; Wang, J.; Huang, W. "The formation of perovskite multiple quantum well structures for high performance

light-emitting diodes". *npj Flexible Electronics* **2018**, 2, 12

63. Lee, S.; Park, J. H.; Nam, Y. S.; Lee, B. R.; Zhao, B.; Nuzzo, D. D.; Jung, E. D.; Jeon, H.; Kim, J.-Y.; Jeong, H. Y.; Friend, R. H.; Song, M. H. "Growth of Nanosized Single Crystals for Efficient Perovskite Light-Emitting Diodes". *ACS Nano* **2018**, 12 (4), 3417-3423
64. Cao, Y.; Wang, N.; Tian, H.; Guo, J.; Wei, Y.; Chen, H.; Miao, Y.; Zou, W.; Pan, K.; He, Y.; Cao, H.; Ke, Y.; Xu, M.; Wang, Y.; Yang, M.; Du, K.; Fu, Z.; Kong, D.; Dai, D.; Jin, Y.; Li, G.; Li, H.; Peng, Q.; Wang, J.; Huang, W. "Perovskite light-emitting diodes based on spontaneously formed submicrometre-scale structures". *Nature* **2018**, 562, 249–253
65. Zhao, B.; Bai, S.; Kim, V.; Lamboll, R.; Shivanna, R.; Auras, F.; Richter, J. M.; Yang, L.; Dai, L.; Alsari, M.; She, X.-J.; Liang, L.; Zhang, J.; Lilliu, S.; Gao, P.; Snaith, H. J.; Wang, J.; Greenham, N. C.; Friend, R. H.; Di, D. "High-efficiency perovskite–polymer bulk heterostructure light-emitting diodes". *Nature Photonics* **2018**, 12, 783-789
66. Yang, M; Wang, N; Zhang, S; Zou, W; He, Y; Wei, Y; Xu, M; Wang, J; Huang, W. "Reduced efficiency roll-off and enhanced stability in perovskite light-emitting diodes with multiple quantum wells". *The Journal of Physical Chemistry Letters* **2018**, 9 (8), 2038–2042
67. Ke, Y.; Wang, N.; Kong, D.; Cao, Y.; He, Y.; Zhu, L.; Wang, Y.; Xue, C.; Peng, Q.; Gao, F.; Huang, W.; Wang, J. "Defect Passivation for Red Perovskite Light-Emitting Diodes with Improved Brightness and Stability". *The Journal of Physical Chemistry Letters* **2019**, 10 (3), 380-385
68. Shin, Y. S.; Yoon, Y. J.; Lee, K. T.; Jeong, J.; Park, S. Y.; Kim, G.-H.; Kim, J. Y. "Vivid and Fully Saturated Blue Light-Emitting Diodes Based on Ligand-Modified Halide Perovskite Nanocrystals". *ACS Applied Materials & Interfaces* **2019**, 11 (26), 23401–23409
69. Chiba, T.; Hoshi, K.; Pu, Y.-J.; Takeda, Y.; Hayashi, Y.; Ohisa, S.; Kawata, S.; Kido, J. "High-Efficiency Perovskite Quantum-Dot Light-Emitting Devices by Effective Washing Process and Interfacial Energy Level Alignment". *ACS Applied Materials & Interfaces* **2017**, 9 (21), 18054–18060
70. Hou, S.; Gangishetty, M. K.; Quan, Q.; Congreve, D. N.; "Efficient Blue and White Perovskite Light-Emitting Diodes via Manganese Doping". *Joule* **2018**, 2 (11), 2421-2433
71. Lee, J. K.; Ma, W. L.; Brabec, C. J.; Yuen, J.; Moon, J. S.; Kim, J. Y.; Lee, K.; Bazan, G. C.; Heeger, A. J. "Processing Additives for Improved Efficiency from Bulk Heterojunction Solar Cells". *Journal of the American Chemical Society* **2008**, 130 (11), 3619–3623
72. Kim, Y.-H.; Cho, H.; Lee, T.-W. "Metal halide perovskite light emitters". *Proceedings of the National Academy of Sciences of the United States of America* **2016**, 113 (42), 11694-1170

Acknowledgement

For 2 years, there have been many people who helped me to complete my MS research. It is my pleasure to thank them. Among them, I want to sincerely thank my advisor, prof. Jin Young Kim, for his advice and instruction with his ardor and patience. Every time he gave me chances to study what I really wanted to. He helped me to go forward in the right direction. I also appreciate my committee members, prof. Myoung Hoon Song and prof. Gi-Hwan Kim who told me professional advice.

I would like to say thank you to my laboratory NGEL members, Hye Rim Yeom, Jaeki Jeong, Hak-beom Kim, Seyoung Song, Jungwoo Heo, Song Yi Park, Tack Ho Lee, Kang Take Lee, Yung Jin Yoon, Na Gyeong An, Jae Won Kim, Hyungsu Jang, Yun Seop Shin, Hye Won Cho, Jiwoo Yeop, Jongdeuk Seo, Woojin Lee, Dohun Yuk, Jung Geon Son, Chan Beom Park, and Taehee Song. Especially, I would like to thank LED team members who gave me many ideas and advice when I meet with a difficulty. Yung Jin led me in the beginning of my research and assist me as a senior. Yun Seop taught me to analyze the result of experiment when we use TCSPC and PL equipment. Chan Beom prepared PeNCs solution for the LEDs device. Also, Jae Won and Hye Won helped me to measure AFM. Song Yi told me advice about fabricating SCLC device. Lastly, I would like to thank my family and would like to express my love to Uiryang.

Finally, I could finish my MS program thanks to all the people who helped and supported me. I will try my best after the graduation with these experience as a steppingstone.